Supplemental Figure 1

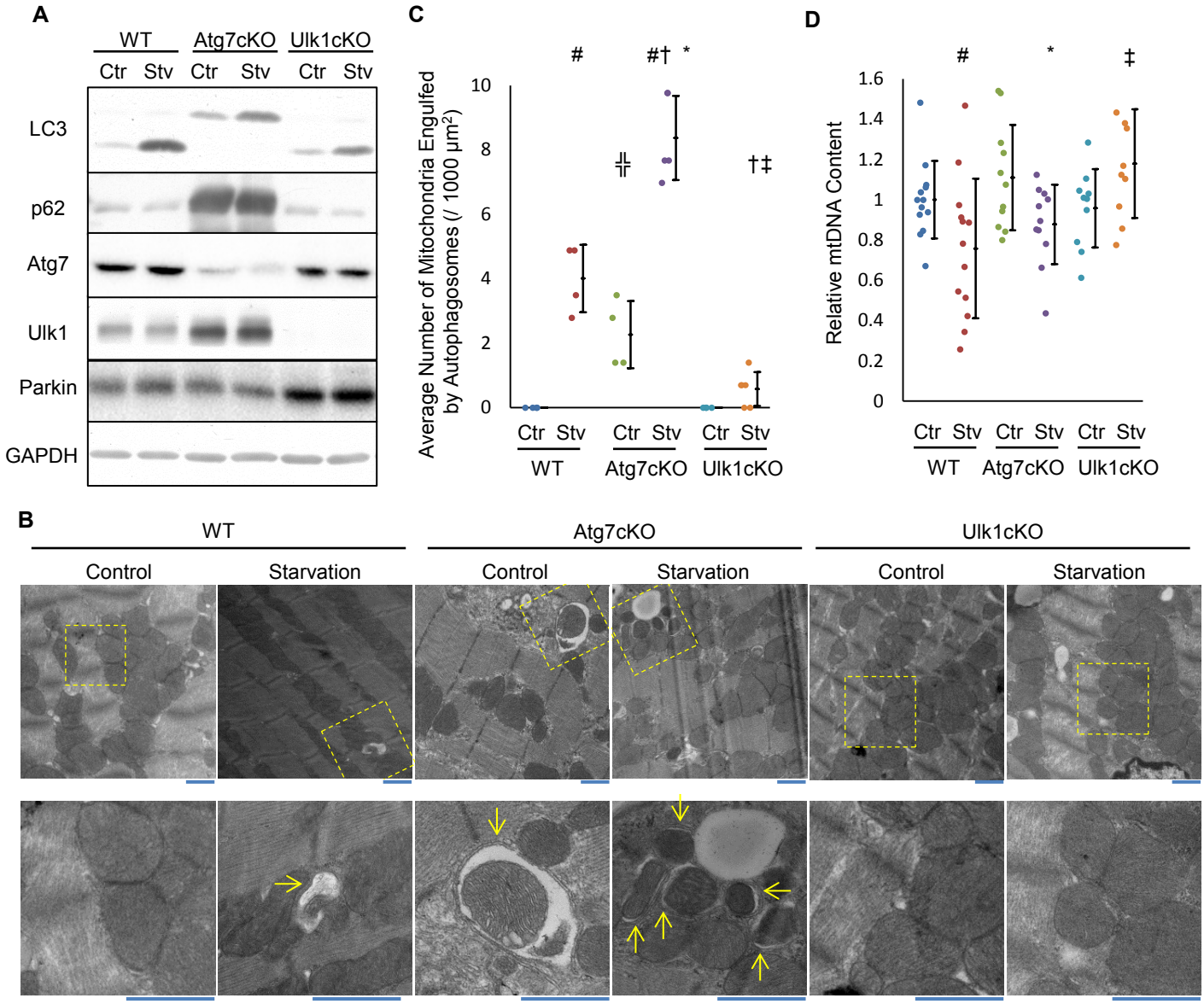

Supplemental Figure 1.

Mice were subjected to 48-hour starvation. Ctr: control, Stv: starvation. Error bars represent SD.

(A) Protein levels of indicated proteins in the heart were analyzed.

(B, C) Mitophagy in the heart was examined by electron microscopy. The mitochondria in autophagosomes were distinguished by the preserved cristae structure. Representative images are shown in (B) (scale bar, 1 μm). Arrows (→) indicate double membrane structures representing autophagosomes. Summary is shown in (C) (n=4-6 per group). Ten fields (1433.9 μm^2) were selected randomly for each mouse heart. The number of mitochondria engulfed by autophagosomes was counted. #$p<0.01$ vs. WT/Ctr; ╬$p<0.05$ vs. WT/Ctr; †$p<0.01$ vs. WT/Stv; *$p<0.01$ vs. Atg7cKO/Ctr; ‡$p<0.01$ vs. Atg7cKO/Stv (Tukey-Kramer's test).

(D) Relative mitochondrial DNA (mtDNA) content in the heart was analyzed by quantitative PCR (n=10-13 per group). #$p<0.05$ vs. WT/Ctr; *$p<0.05$ vs. Atg7cKO/Ctr; ‡$p<0.05$ vs. Ulk1cKO/Ctr (Student's t-test (unpaired)).

Supplemental Figure 1

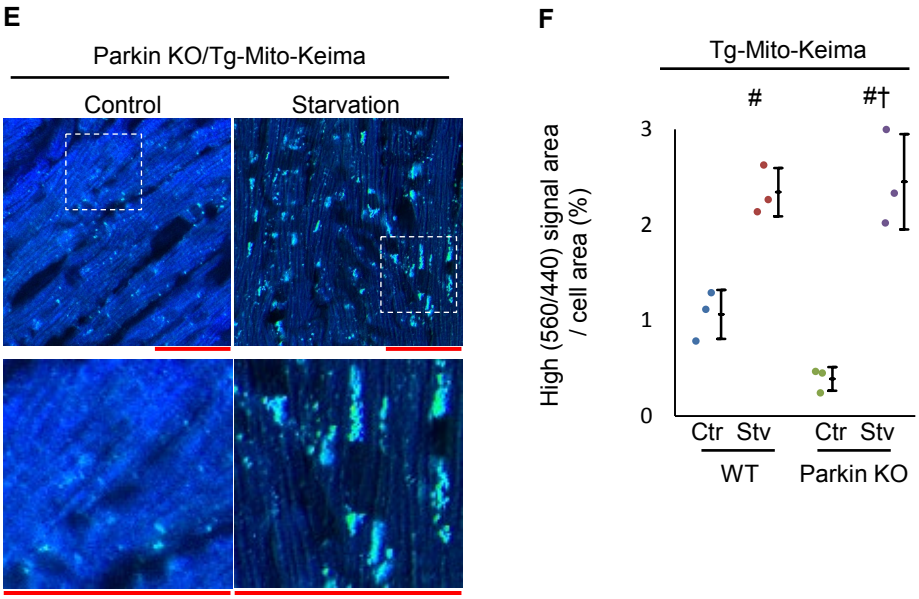

Supplemental Figure 1. Continued.

(E, F) Lysosomal degradation of mitochondria was examined in the hearts of Tg-Mito-Keima mice during starvation. Representative images are shown in (E) (scale bar, 50 μm). Summary is shown in (F) (n=3 per group). #p<0.01 vs. WT/Ctr, †p<0.01 vs. Parkin KO/Ctr (Tukey-Kramer's test).

Supplemental Figure 2

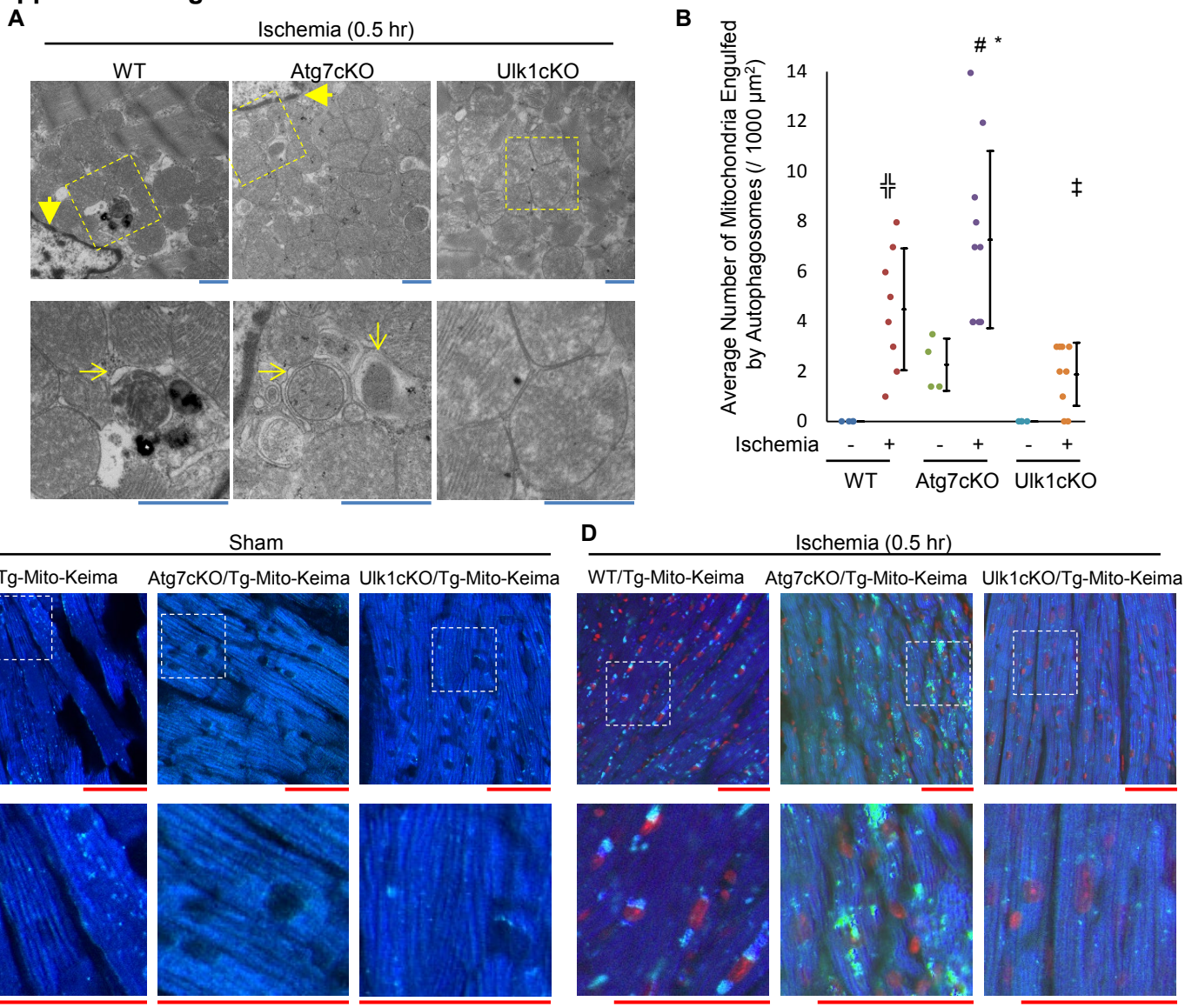

Supplemental Figure 2.

(A-G) Mice were subjected to prolonged ischemia. Hearts were excised at indicated time points after coronary artery ligation. Error bars represent SD.

(A, B) Mitophagy in the heart was examined by electron microscopy. The mitochondria in autophagosomes were distinguished by the preserved cristae structure. Representative images are shown in (A) (scale bar, 1 μm). Arrows (→) and arrow heads (▲) indicate double membrane structures representing autophagosomes and nucleus, respectively. Summary is shown in (B) (n=8-10 per group). Seven fields (1008.7 μm^2) were selected randomly for each mouse heart. The number of mitochondria engulfed by autophagosomes was counted. ╬p<0.05 vs. WT/Ischemia(-); #p<0.01 vs. WT/Ischemia(-); *p<0.01 vs. Atg7cKO/Ischemia(-); ‡p<0.01 vs. Atg7cKO/Ischemia(+) (Tukey-Kramer's test).

(C, D) Lysosomal degradation of mitochondria was examined in the hearts of Tg-Mito-Keima mice during ischemia (scale bar, 50 μm). Representative images in Sham Group are shown in (C). Representative images with nuclear staining are shown in (D). Nuclei are tracked by red color.

Supplemental Figure 2

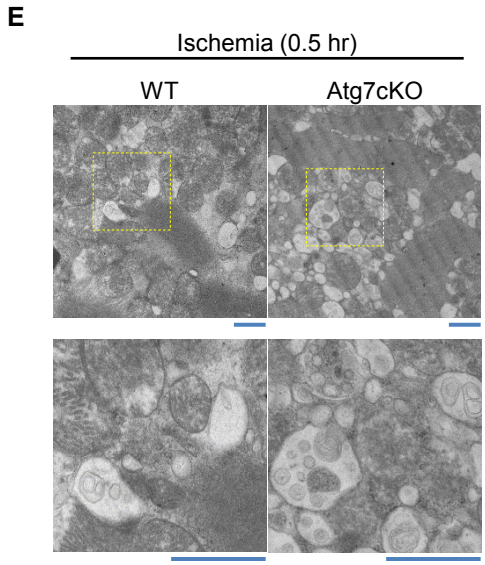

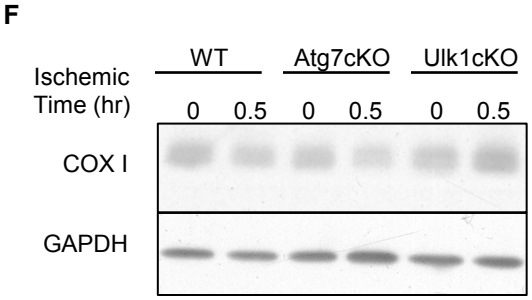

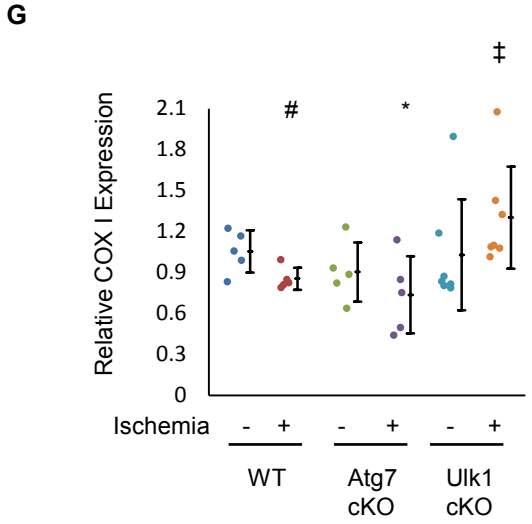

Supplemental Figure 2. Continued.

(E) Lysosomal degradation of organelles in the heart was observed by electron microscopy. Enlarged images are shown below (scale bar, 1 μm).

(F, G) Protein levels of COX I in the heart were analyzed. Representative immunoblots are shown in (F). Summary is shown in (G) (n=5-7 per group). #p<0.05 vs. WT/Ischemia(-); *p<0.05 vs. Atg7cKO/Ischemia(-); ‡p<0.05 vs. Ulk1cKO/Ischemia(-) (Student's t-test (paired)).

Supplemental Figure 3

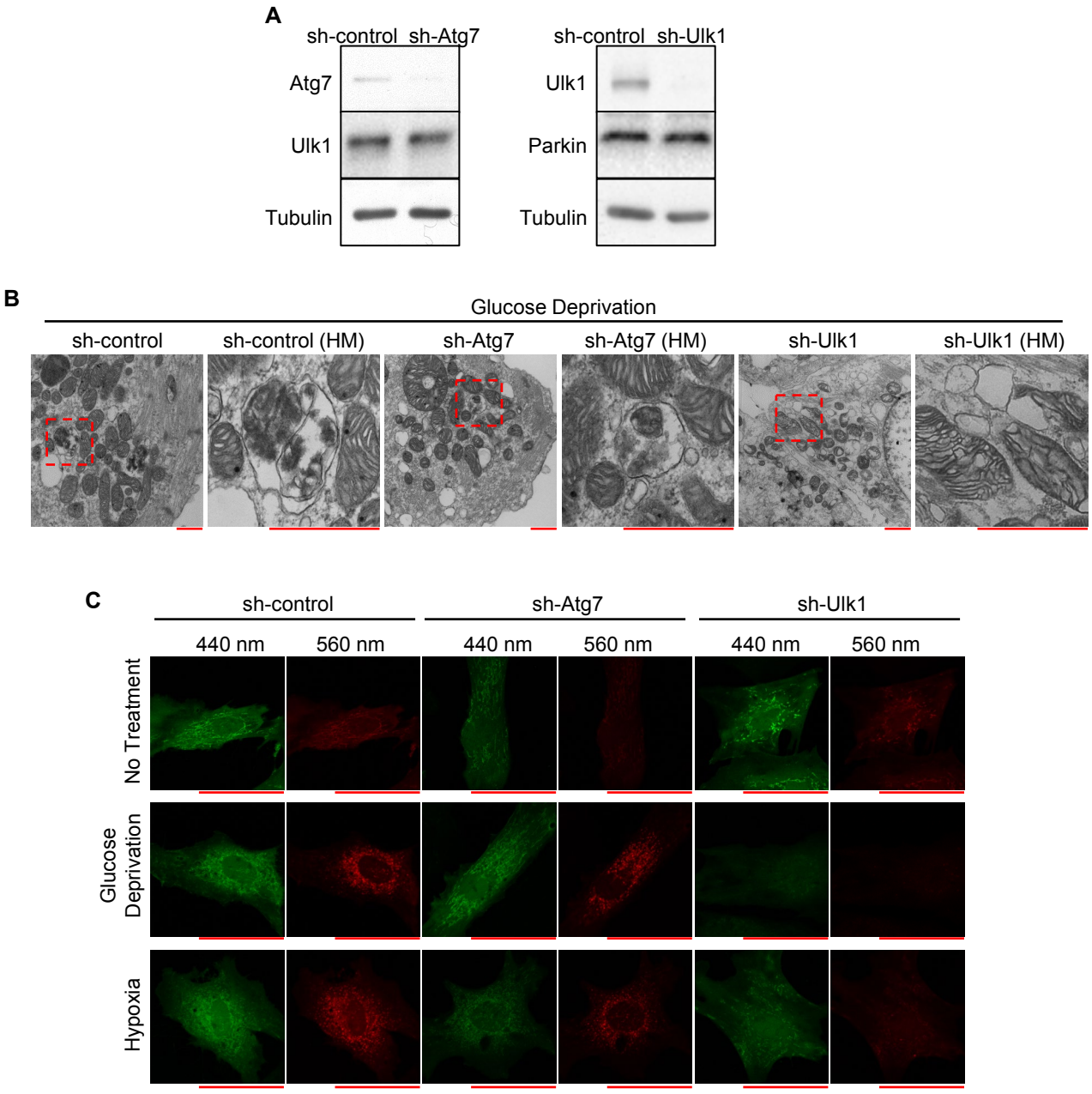

Supplemental Figure 3.

(A) Representative immunoblots showing the knockdown of Atg7 or Ulk1. Ulk1 (left panel) and Parkin (right panel) were detected on a parallel gel.

(B) Representative electron micrographs of the CMs (scale bar, 0.5 μm). Demarcation indicates location of area shown under higher magnification.

(C) Images of Mito-Keima at 440 nm and 560 nm corresponding to the images of Mito-Keima with high ratio in Figure 3A (scale bar, 50 μm).

Supplemental Figure 3

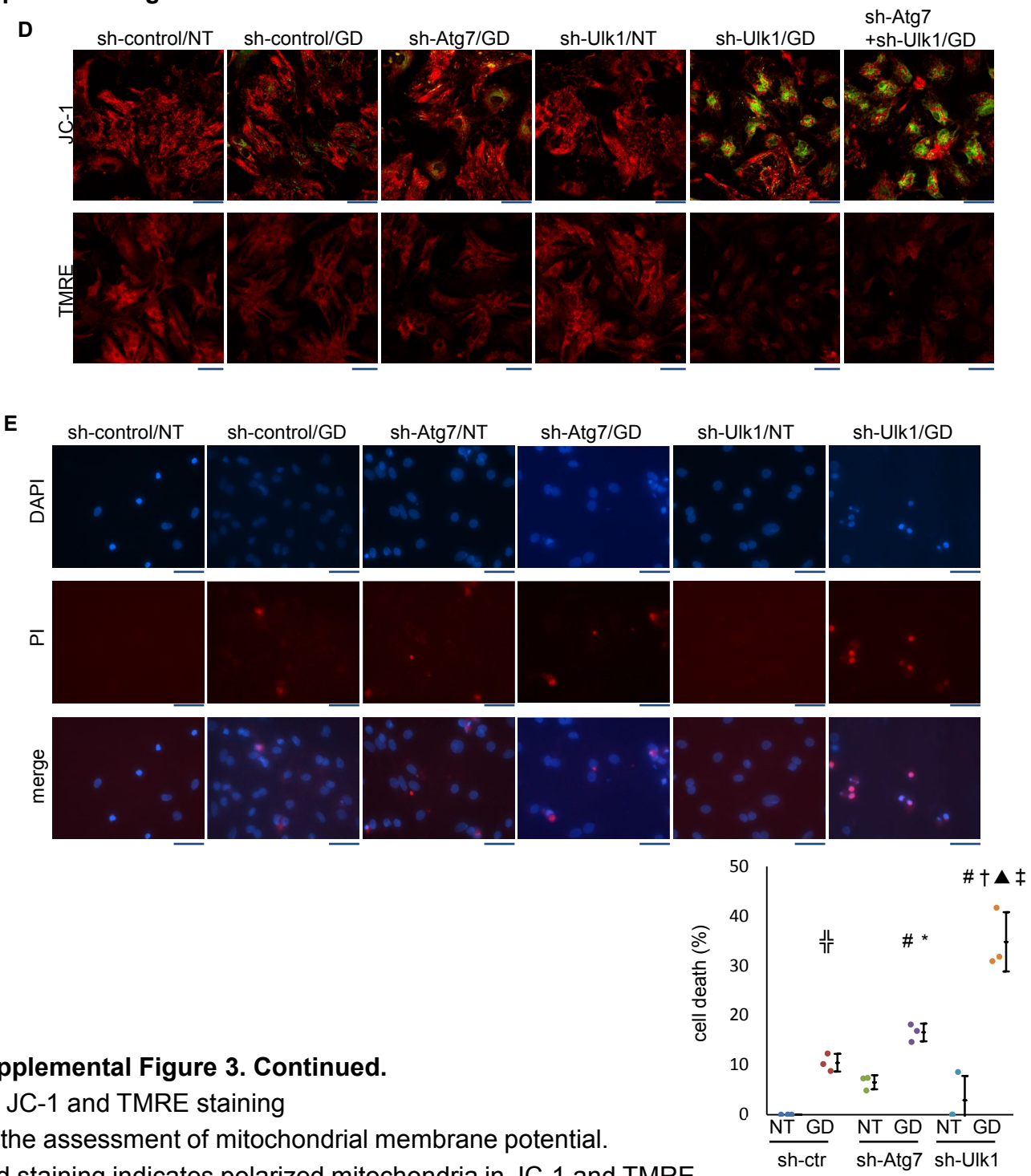

Supplemental Figure 3. Continued.

(D) JC-1 and TMRE staining
for the assessment of mitochondrial membrane potential.
Red staining indicates polarized mitochondria in JC-1 and TMRE.
Green staining indicates depolarized mitochondria in JC-1 (scale bar, 50 μm).
(E) Propidium iodide (PI) nucleic acid staining for the assessment of cell death. Glucose deprivation (GD) was applied for 6 hours. Representative images of DAPI (blue) and PI (red) staining are shown in upper panel (scale bar, 50 μm). A summary is shown in lower panel (n=3 per group). Error bars represent SD. ╬p<0.05 vs sh-ctr/NT; #p<0.01 vs. sh-ctr/NT; *p<0.05 vs. sh-Atg7/NT; †p<0.01 vs. sh-ctr/GD; ▲p<0.01 vs. sh-Atg7/GD; ‡p<0.01 vs. sh-Ulk1/NT (Tukey-Kramer's test).

Supplemental Figure 3

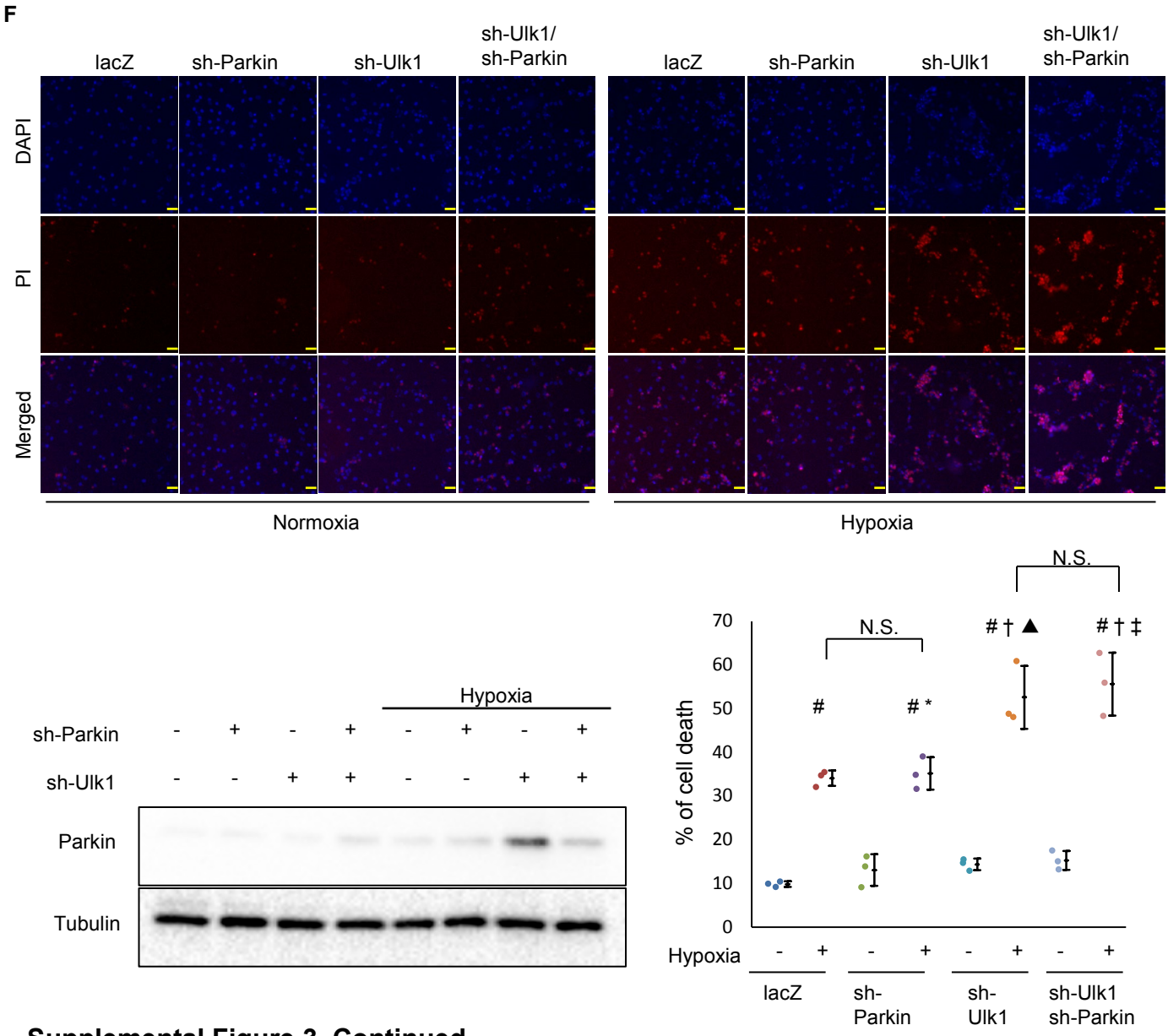

Supplemental Figure 3. Continued.

(F) Propidium iodide (PI) nucleic acid staining for the assessment of cell death. Hypoxia was applied for 4 hours. Representative images of DAPI (blue) and PI (red) staining are shown in the upper panel (scale bar, 50 μm). Representative immunoblots showing the effect of hypoxia upon Parkin expression in CMs transduced with sh-Ulk1 are shown in the lower left panel. Quantification and statistical analysis are shown in the lower right panel (n=3 per group). Error bars represent SD. N.S. Not significant; #p<0.01 vs. lacZ/Normoxia; †p<0.01 vs. lacZ/Hypoxia; *p<0.01 vs. sh-Parkin/Normoxia; ▲p<0.01 vs. sh-Ulk1/Normoxia; ‡p<0.01 vs. sh-Ulk1/sh-Parkin/Normoxia (Tukey-Kramer's test).

.

Supplemental Figure 3

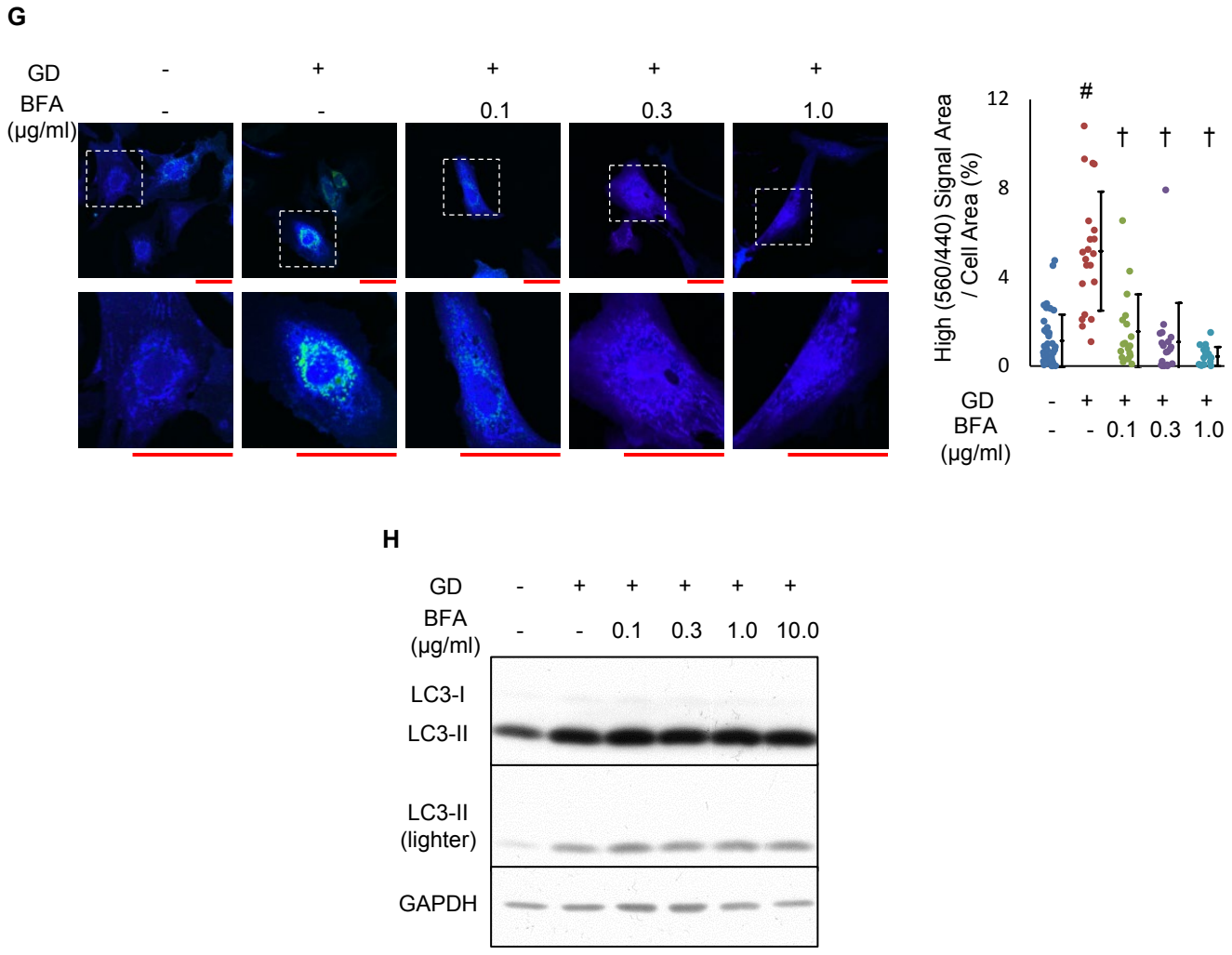

Supplemental Figure 3. Continued.

(G) Mitophagy was examined in CMs transduced with Mito-Keima after 4 hours of GD. Brefeldin A (BFA) was applied during GD at indicated concentrations.

Left: Representative images showing the high ratio dots. Enlarged images are shown below (scale bar, 50 μm). Right: Quantitation of the area of high ratio dots per cell area (%).

The cell numbers in each group were 39, 21 (mock) and 18, 19, 18 (BFA) from 3 independent experiments. Error bars represent SD. #p<0.01 vs. GD(-)/BFA(-); †p<0.01 vs. GD(+)/BFA(-) (Tukey-Kramer's test).

(H) Representative immunoblots showing the level of LC3 in the presence or absence of BFA during GD in CMs.

Supplemental Figure 3

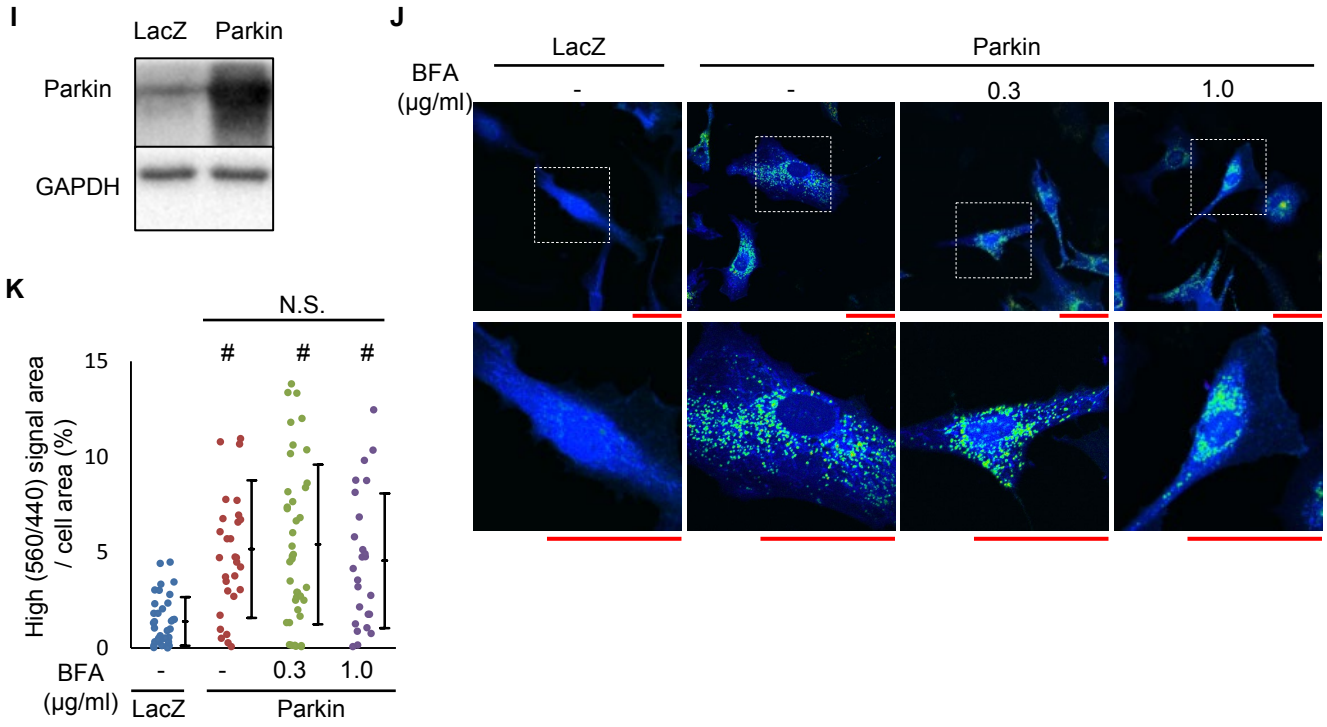

Supplemental Figure 3. Continued.

(I-K) Mitophagy induced by overexpression of Parkin was evaluated in CMs transduced with Mito-Keima.

(I) Representative immunoblots showing overexpression of Parkin.

(J) Representative images showing high ratio dots of Mito-Keima (scale bar, 50 μm).

(K) Quantitation of the area of high ratio dots per cell area (%). The cell numbers in each group were 36 (LacZ) and 30, 40, 25 (Parkin). Error bars represent SD. #p<0.01 vs. LacZ; N.S., not significant (Tukey-Kramer's test).

Supplemental Figure 4

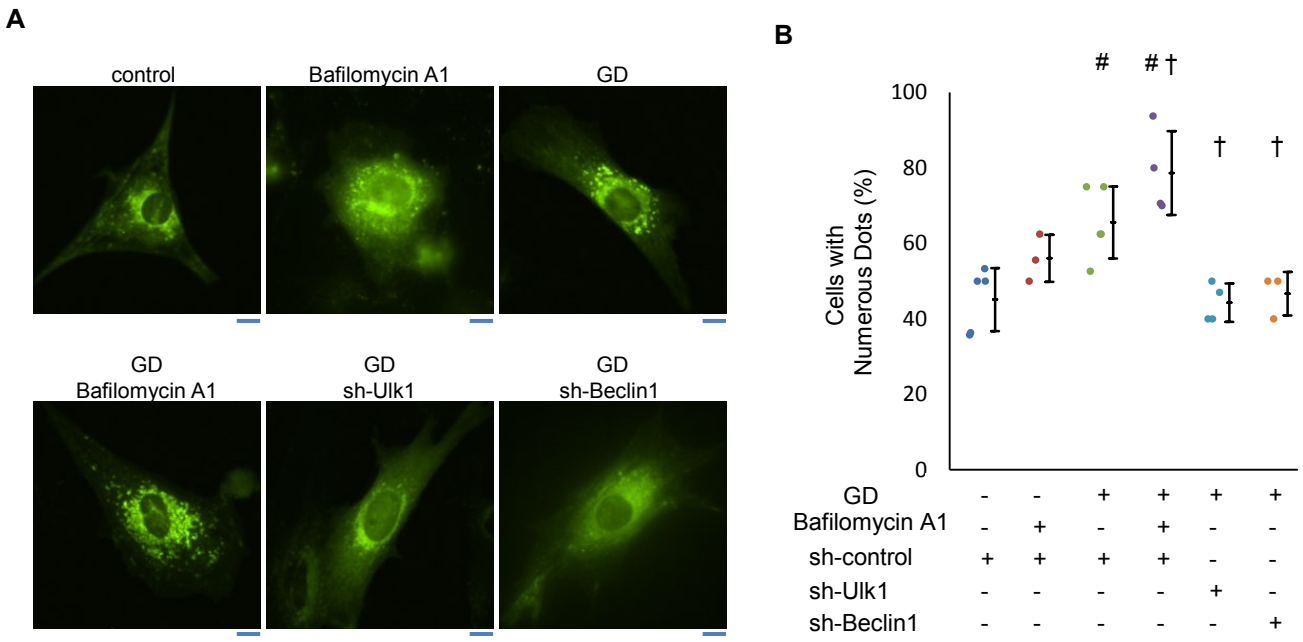

Supplemental Figure 4.

(A, B) YFP-Rab9 puncta were analyzed before and after GD with or without Bafilomycin A1 treatment in CMs transduced with indicated sh-RNAs. Representative images are shown in (A) (scale bar, 10 μm). Summary is shown in (B) (n=3-5 per group). Cells with more than 20 dots were counted. Error bars represent SD. #p<0.05 vs. sh-control/GD(-); †p<0.05 vs. sh-control/GD(+) (Student's t-test (unpaired)).

Supplemental Figure 4

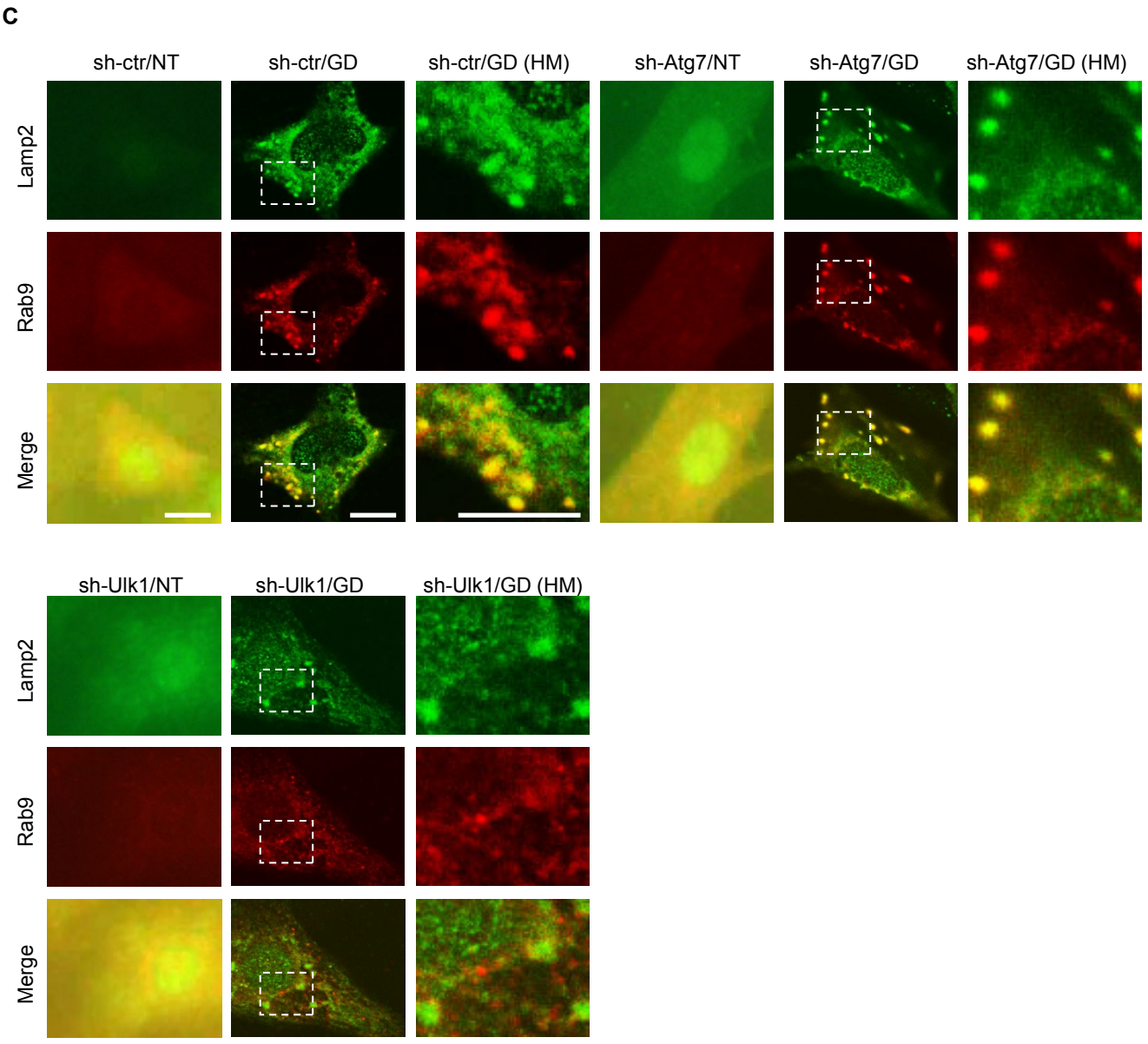

Supplemental Figure 4. Continued.

(C) Representative images of Lamp2 (green) and Rab9 (red) immunohistochemistry after glucose deprivation. Scale bar, 20 μm. Demarcation indicates location of area shown under higher magnification.

Supplemental Figure 4

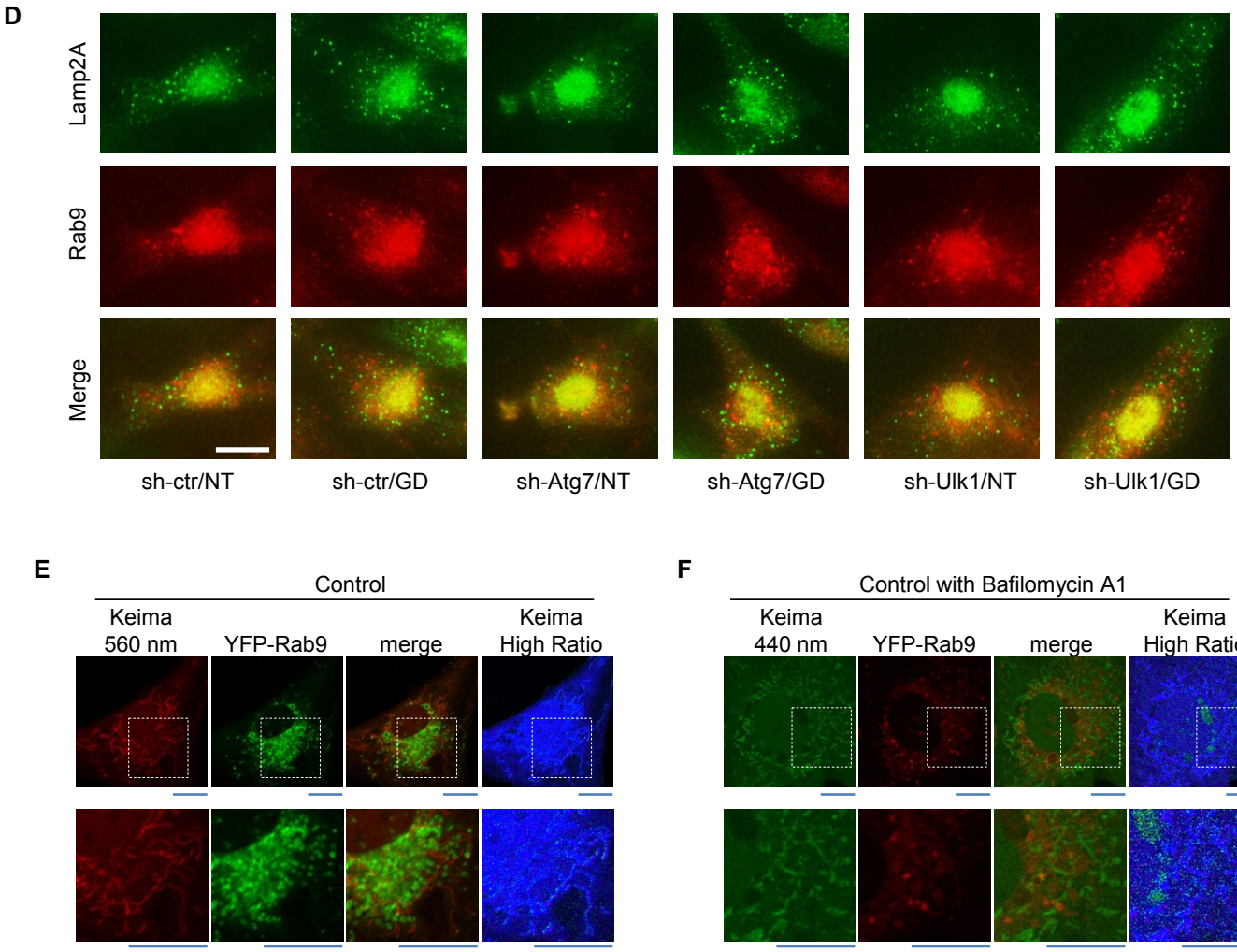

Supplemental Figure 4. Continued.

(D) Representative images of Lamp2A (green) and Rab9 (red) immunohistochemistry. Scale bar, 20 μm.

(E, F) Representative confocal micrographs of CMs transduced with Mito-Keima and YFP-Rab9 at baseline alone or with Bafilomycin A1 treatment ((E) and (F), respectively). Enlarged images are shown below (scale bar, 10 μm).

Supplemental Figure 4

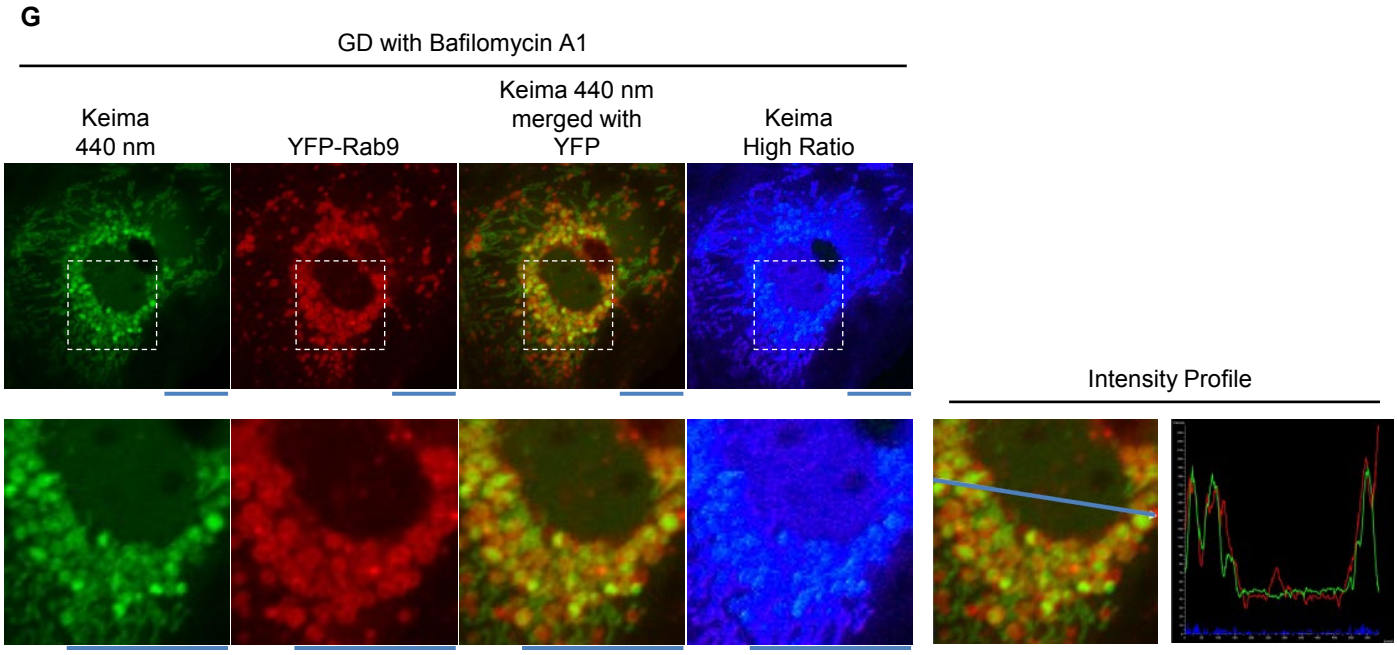

Supplemental Figure 4. Continued.

(G) Representative confocal micrographs of CMs transduced with Mito-Keima and YFP-Rab9 during glucose deprivation with Bafilomycin A1 treatment. Enlarged images are shown below (scale bar, 10 μm). The intensity profile is shown in the two right-most panels. The green line represents the Keima signal (440 nm) while the red line represents the YFP signal.

Supplemental Figure 4

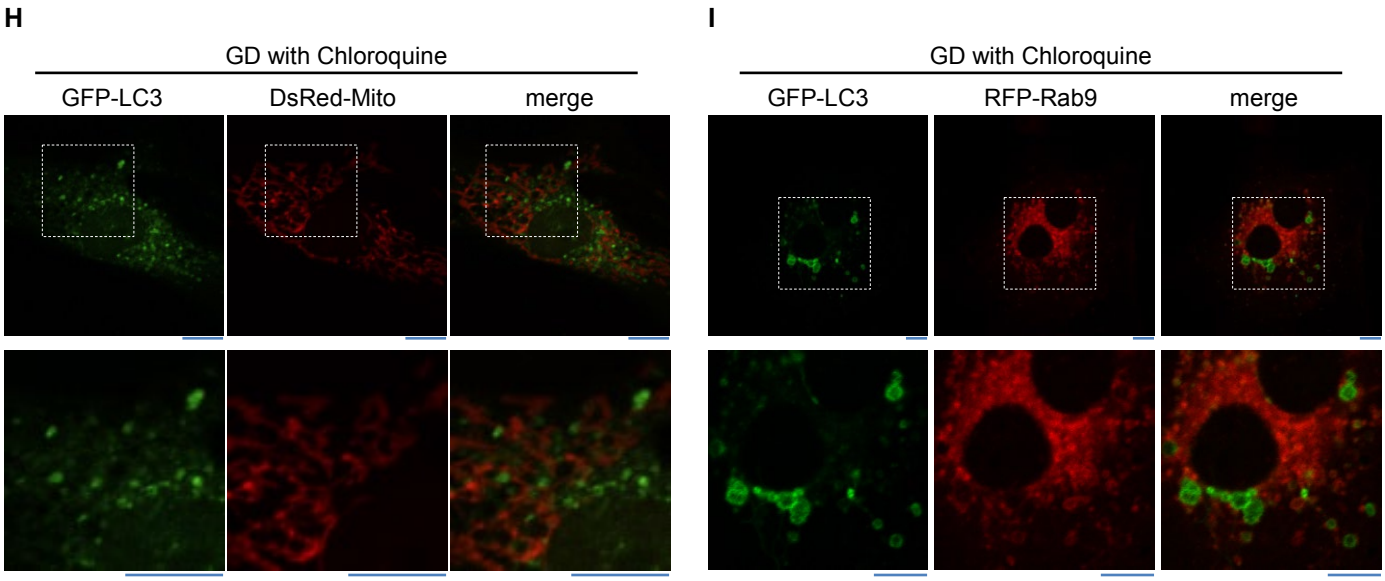

Supplemental Figure 4. Continued.

(H) Representative confocal micrographs of CMs transduced with GFP-LC3 and DsRed-Mito and subjected to GD with chloroquine treatment (scale bar, 10 μm).

(I) Representative confocal micrographs of CMs transduced with GFP-LC3 and RFP-Rab9 and subjected to GD with chloroquine treatment (scale bar, 10 μm).

Supplemental Figure 5

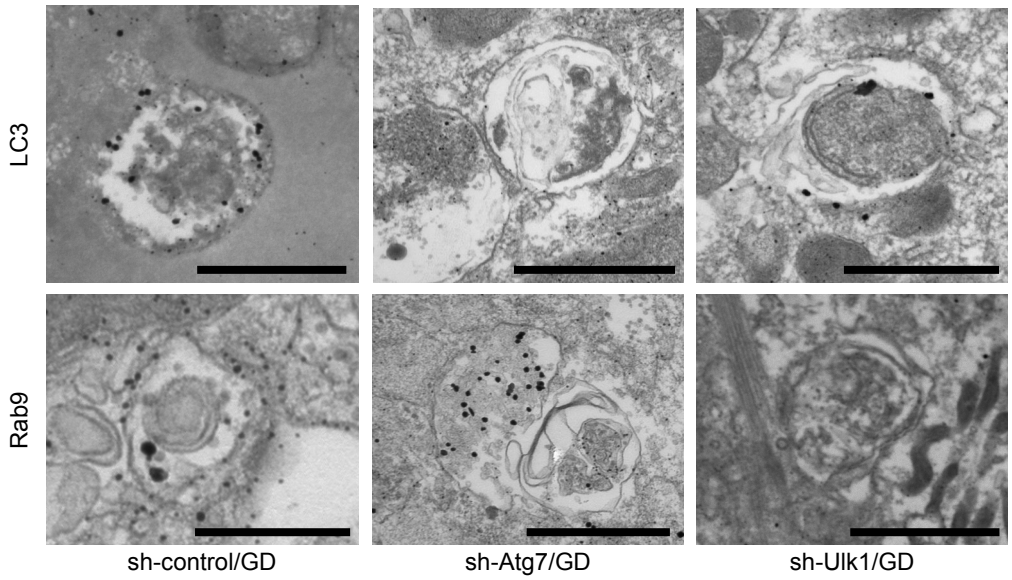

Supplemental Figure 5.
Immuno-Gold EM analyses of autophagosomes in CMs in response to GD. Autophagosomes in Atg7-knockdown CMs were Rab9-positive whereas those in Ulk1-knockdown CMs were LC3-positive (scale bar, 500 nm).

Supplemental Figure 6

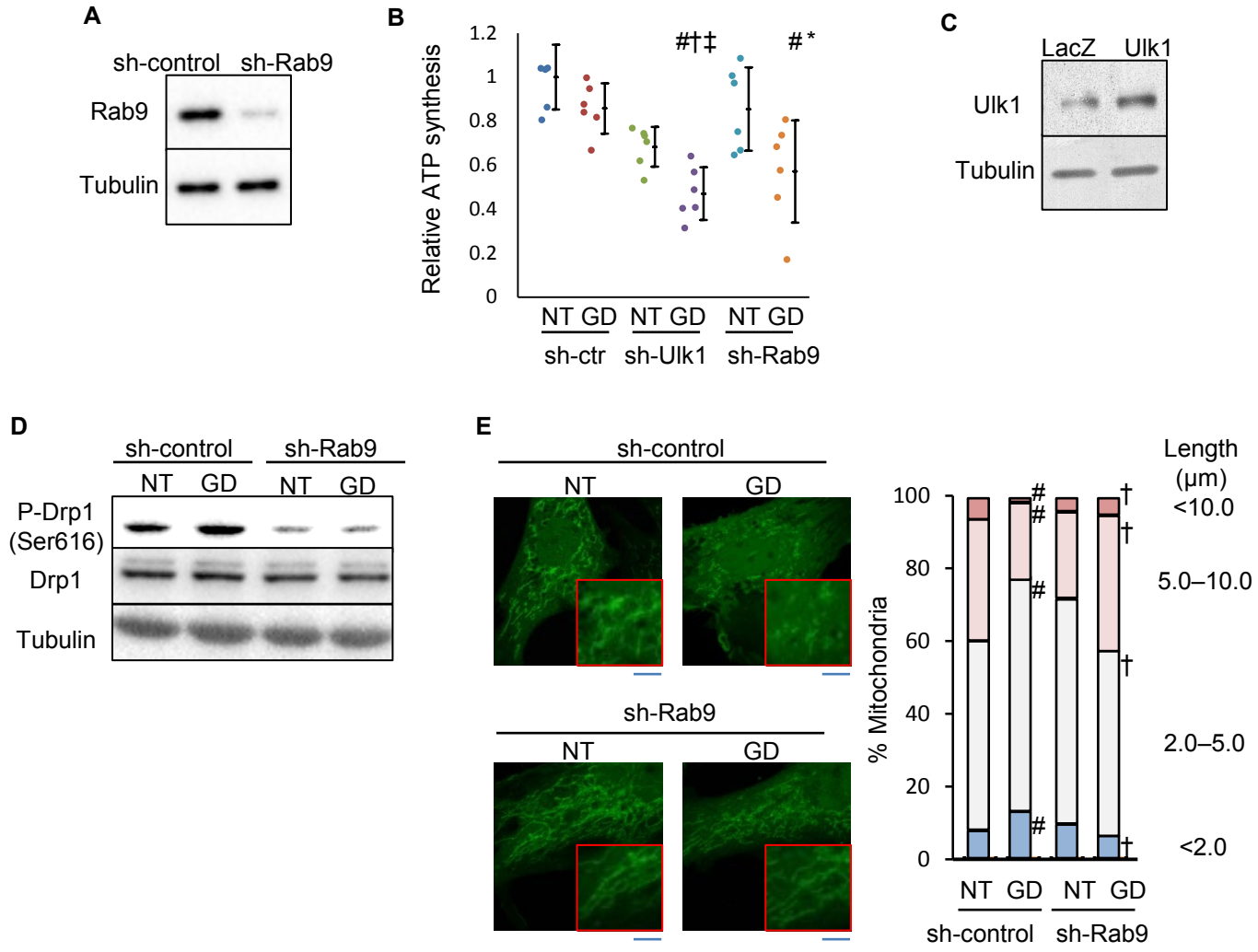

Supplemental Figure 6.

(A) Representative immunoblots showing the knockdown of Rab9.

(B) ATP synthesis in mitochondria isolated from CMs transduced with sh-control, sh-Ulk1 or sh-Rab9 (n=6). Error bars represent SD. #p<0.01 vs. NT/sh-ctr; †p<0.05 vs. GD/sh-ctr; ‡p<0.05 vs. NT/sh-Ulk1; *p<0.01 vs. GD/sh-ctr (Tukey-Kramer's test).

(C) Representative immunoblots showing the overexpression of Ulk1.

(D) Representative immunoblots showing the effect of knockdown of Rab9 upon the phosphorylation of Drp1 at Ser616 during GD.

(E) Mitochondrial length was measured and categorized by size as <2.0, 2.0-5.0, 5.0-10.0 or >10.0 μm in CMs transduced with Mito-Keima. Quantification of mitochondrial length is shown as percentage of total mitochondria. More than 500 cytosolic Mito-Keima points were examined in 10-15 cells from 3 independent experiments for each group. #p<0.05 vs. sh-ctr/NT; †p<0.05 vs. sh-ctr/GD (Student's t-test (unpaired)).

Supplemental Figure 7

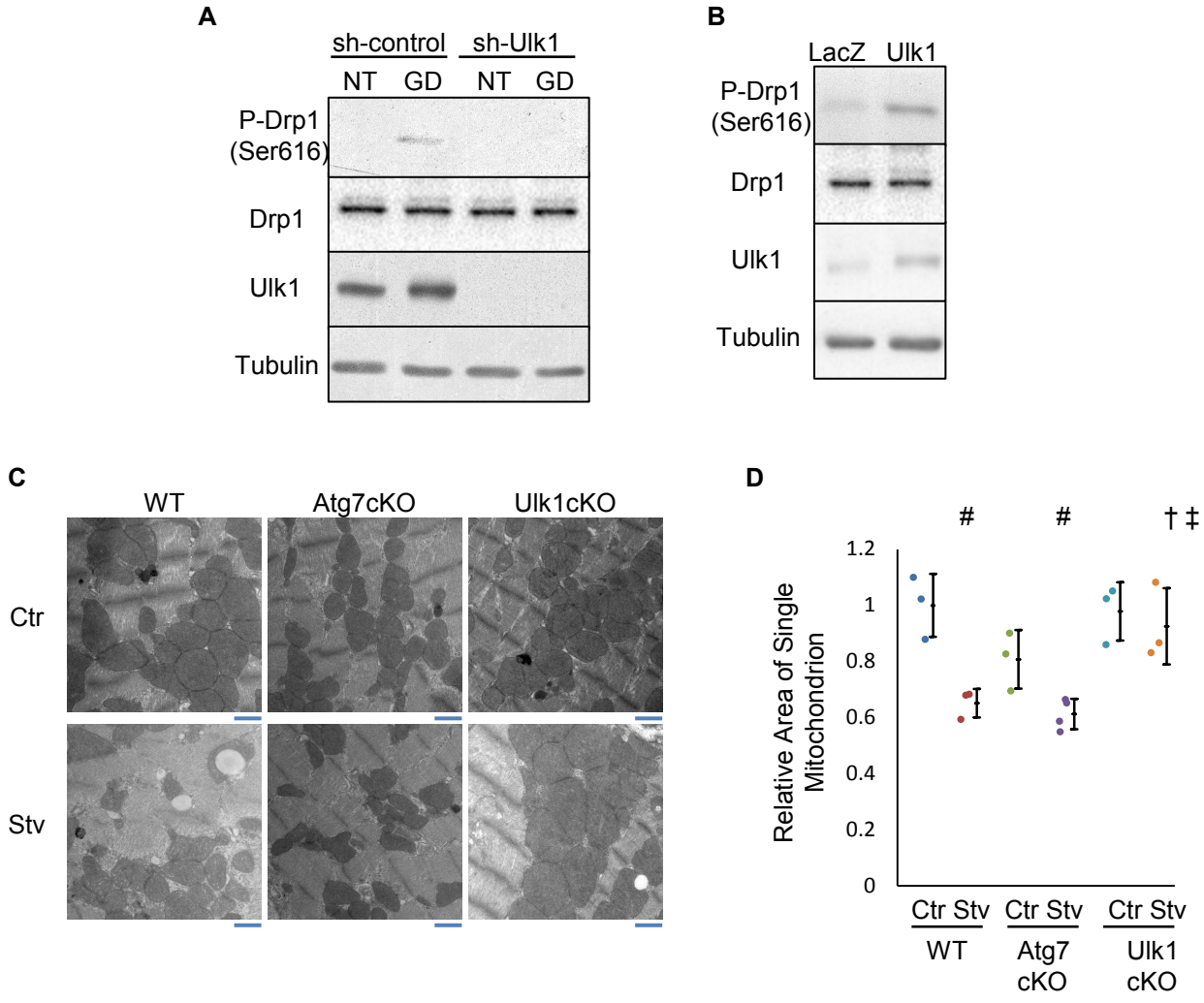

Supplemental Figure 7.

(A) Representative immunoblots showing the effect of knockdown of Ulk1 upon the phosphorylation of Drp1 at Ser616 during GD.

(B) Representative immunoblots showing the effect of overexpression of Ulk1 upon the phosphorylation of Drp1 at Ser616. Drp1 was detected on a parallel gel using the same samples.

(C) Representative electron micrographs of the heart (scale bar, 1 μm).

(D) Quantitation of the average area of a single mitochondrion in the heart.

At least 200 mitochondria were analyzed per mouse (n=3-4 per group). Error bars represent SD. #p<0.01 vs. WT/Ctr; †p<0.05 vs. WT/Stv; ‡p<0.01 vs. Atg7cKO/Stv (Tukey-Kramer's test).

Supplemental Figure 7

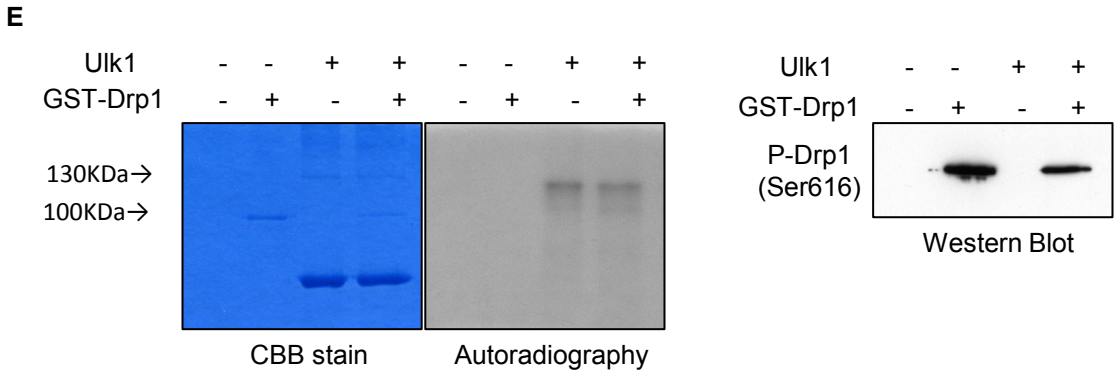

Supplemental Figure 7. Continued.

(E) *In vitro* kinase assays were performed. Ten ng of recombinant Ulk1 (lane 3 and lane 4) and 1 μg of recombinant GST-Drp1 (lane 2 and lane 4) were incubated with ATP at 30^{o}C for 30 minutes. Left: A Coomassie-stained gel. Middle: Autoradiograph. Right: Immunoblot showing the effect of Ulk1 upon the phosphorylation of Drp1 at Ser616 after *in vitro* kinase assay.

Supplemental Figure 7

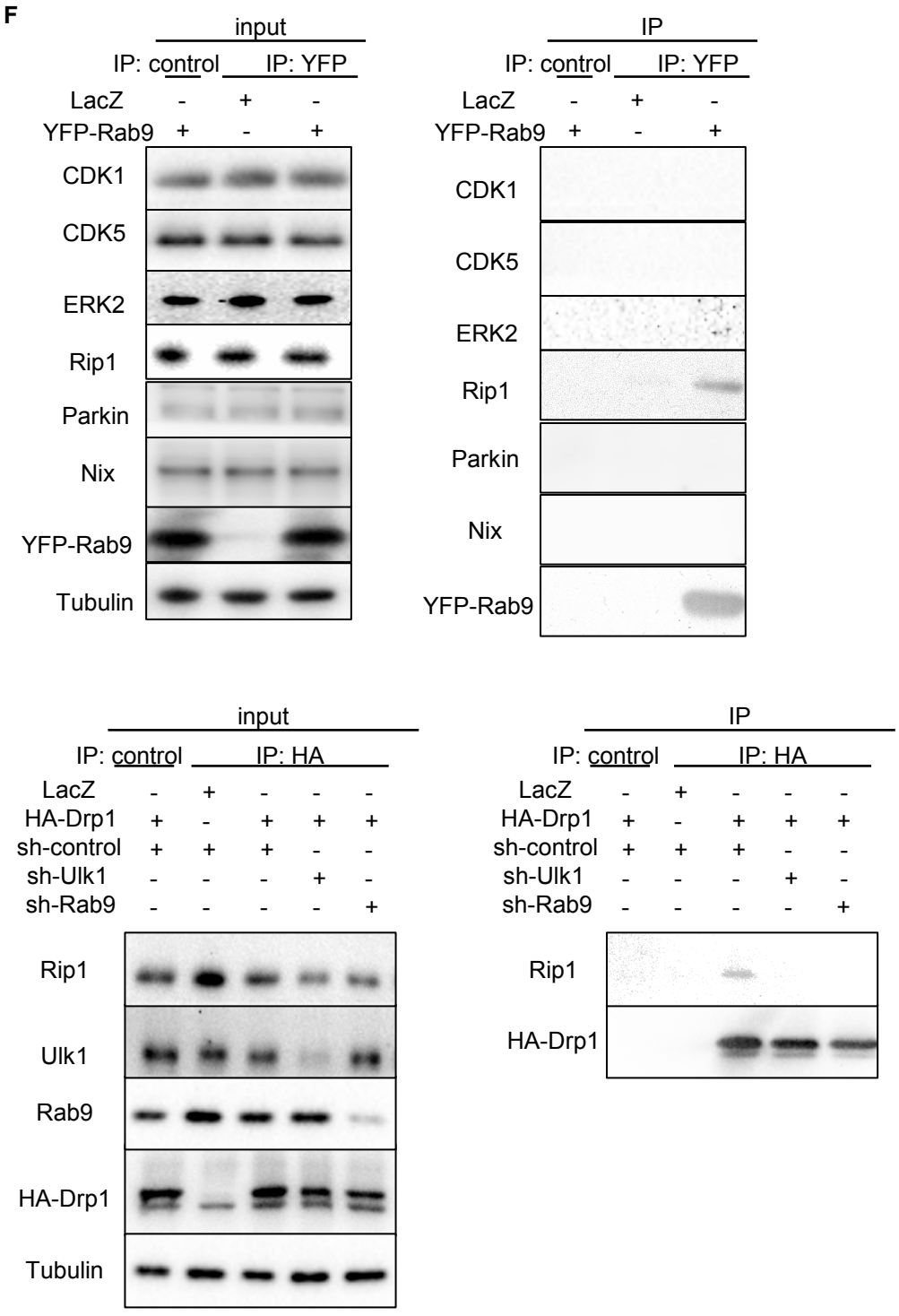

Supplemental Figure 7. Continued.

(F, G) Co-immunoprecipitation was conducted in cardiomyocytes (CMs).

Supplemental Figure 7

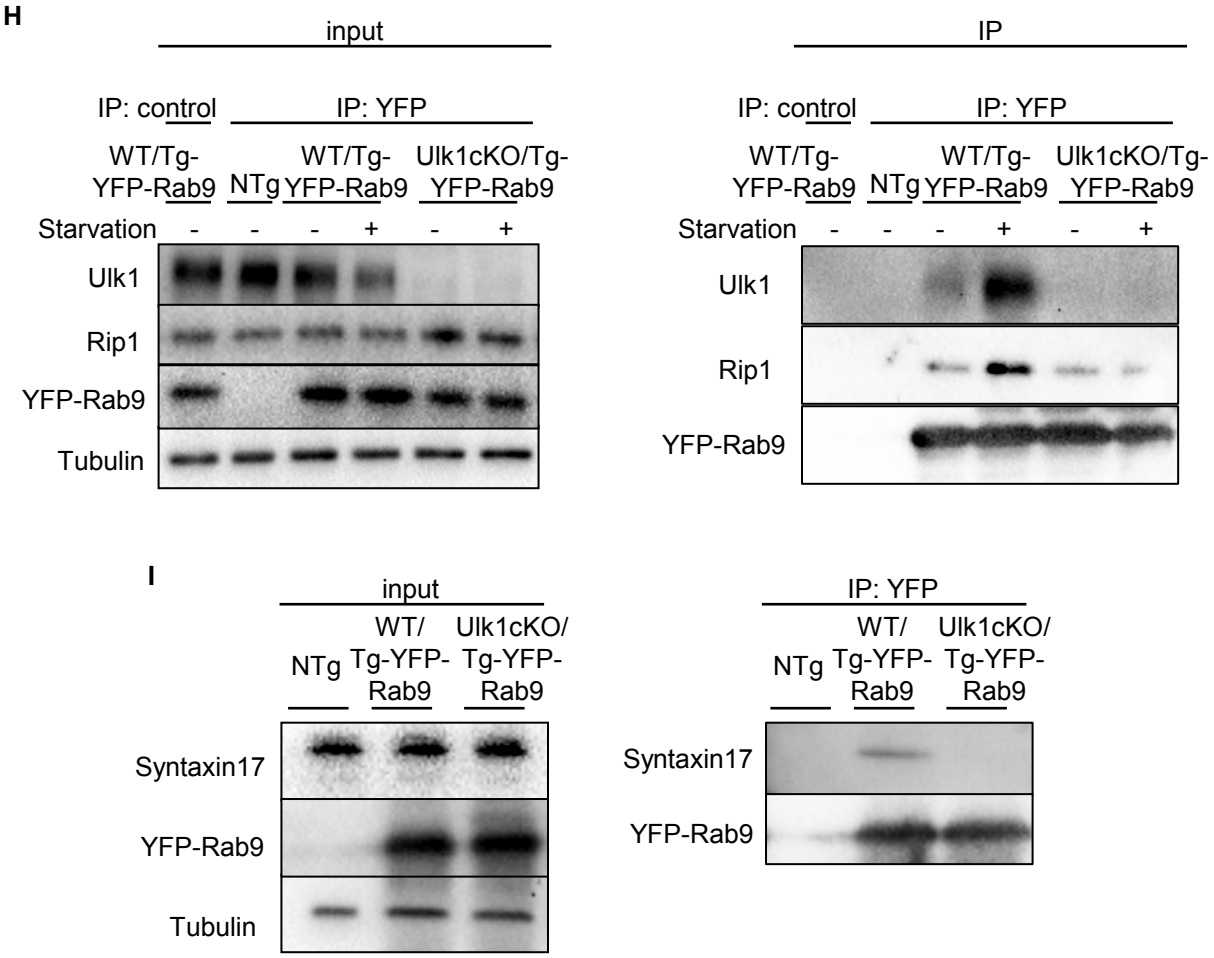

Supplemental Figure 7. Continued.

(H, I) Co-immunoprecipitation was conducted in the hearts of WT/Tg-YFP-Rab9 or Ulk1cKO/ Tg-YFP-Rab9 mice subjected to starvation. In (I), Syntaxin 17 (left panel) was detected on a parallel gel using the same samples.

Supplemental Figure 7

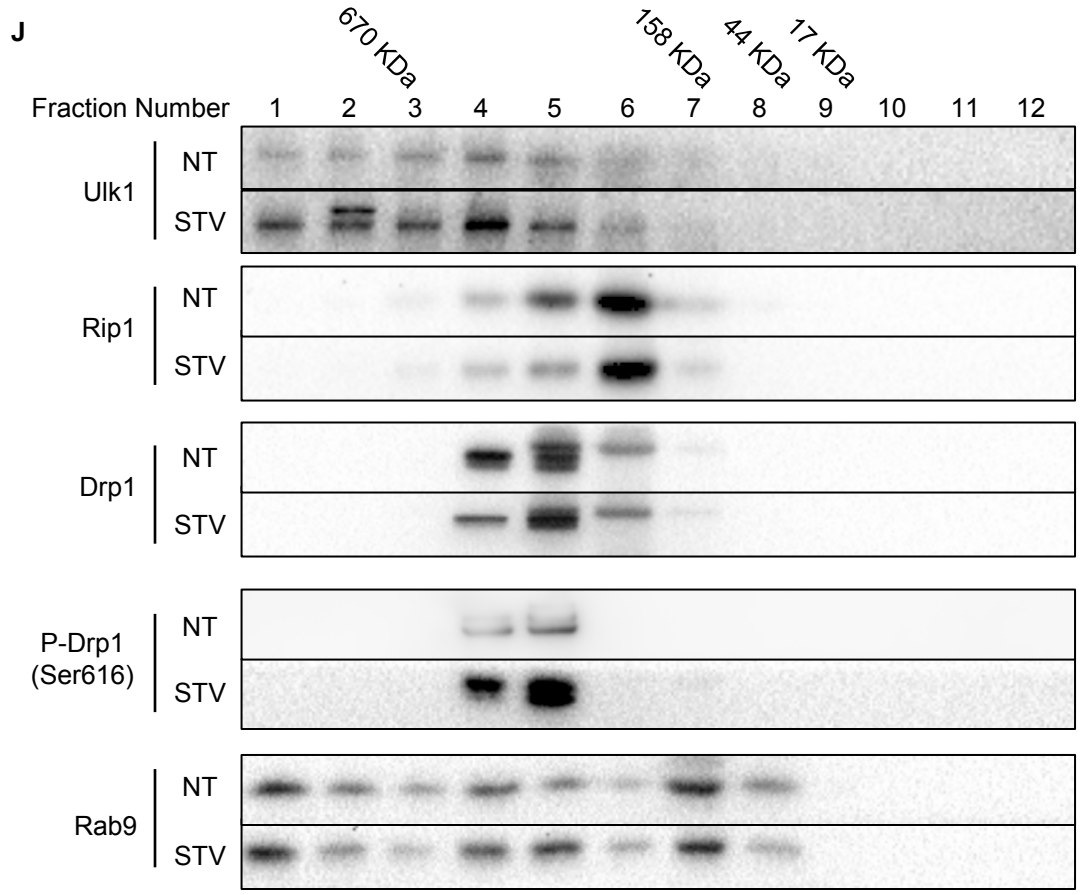

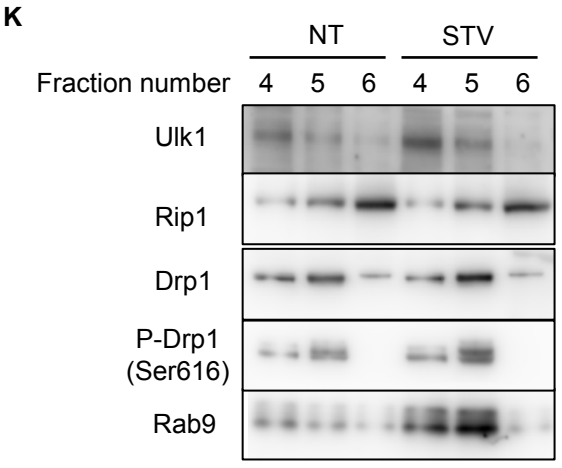

Supplemental Figure 7. Continued.

(J) The heart lysate from WT mice subjected to starvation was assayed using high pressure chromatography and a size exclusion column. Fractions were subjected to immunoblot. Molecular weight standards are indicated above the blot. NT: no treatment, STV: starvation. (K) Fractions #4 to #6 before and after starvation were analyzed on the same gel.

Supplemental Figure 8

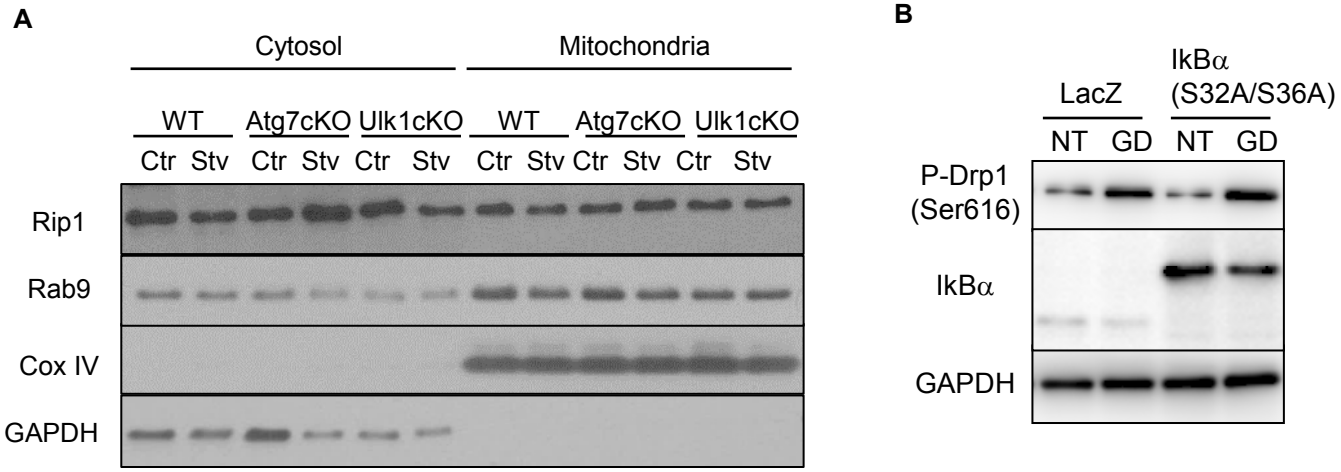

Supplemental Figure 8.

(A) Representative immunoblots of the indicated proteins in the cytosolic and mitochondrial fractions prepared from heart homogenates of the indicated mouse lines.

(B) Phosphorylation of Drp1 at Ser616 was analyzed in the absence or presence of forced expression of IkBα (S32A/S36A) during glucose deprivation. IkBα was detected on a parallel gel using the same samples.

Supplemental Figure 8

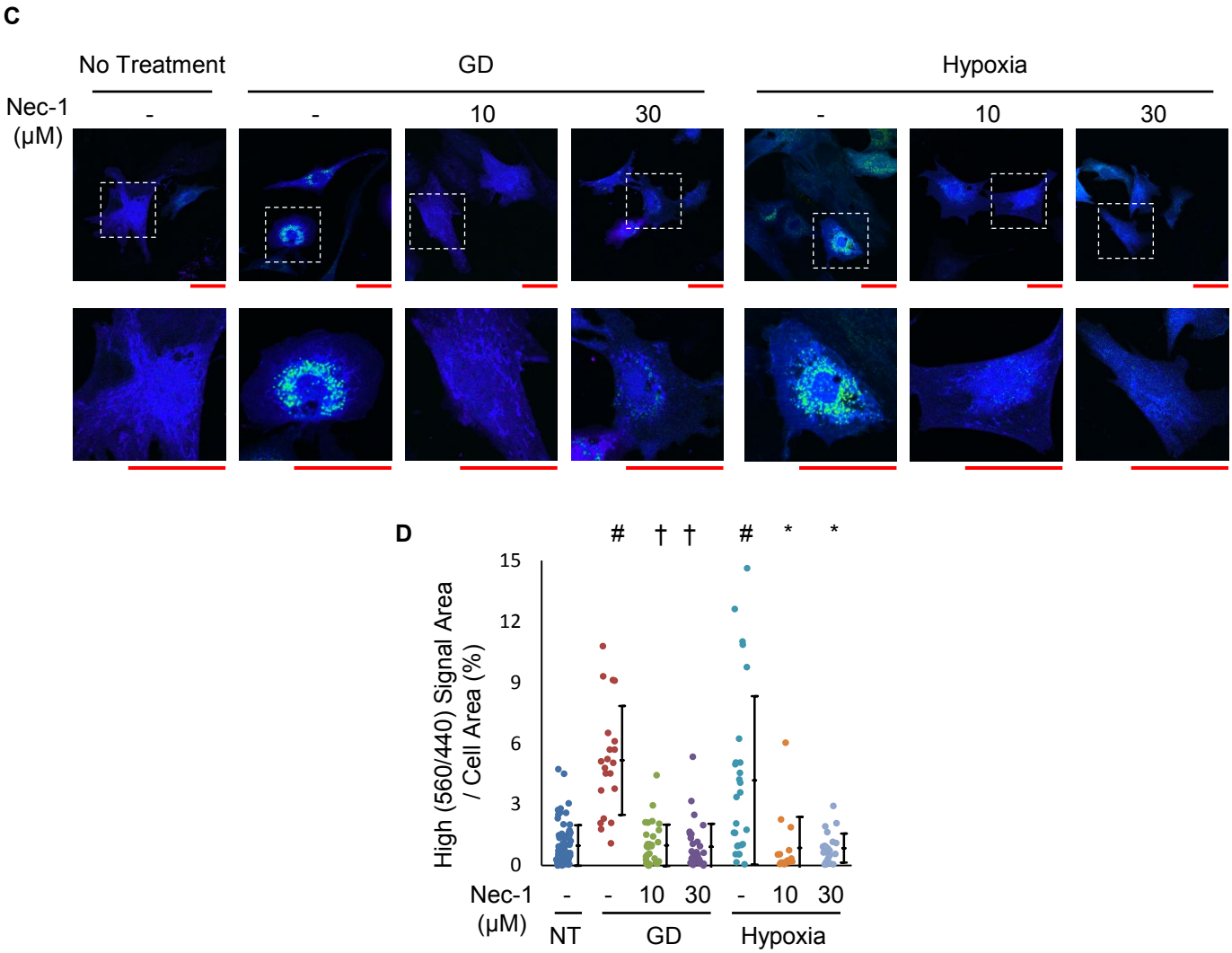

Supplemental Figure 8. Continued.

(C, D) The effect of 7-Cl-O-Nec-1 upon mitophagy was evaluated in CMs transduced with Mito-Keima.

(C) Representative images showing high ratio dots of Mito-Keima (scale bar, 50 μm).

(D) Quantitation of the area of high ratio dots/the total cell area.

The cell numbers in each group were 75 (NT), 21, 22, 21 (GD) and 27, 16, 24 (Hypoxia) from 3 independent experiments. Error bars represent SD. #p<0.01 vs. NT; †p<0.01 vs. GD/Nec-1(-); *p<0.01 vs. Hypoxia/Nec-1(-) (Tukey-Kramer's test).

Supplemental Figure 8

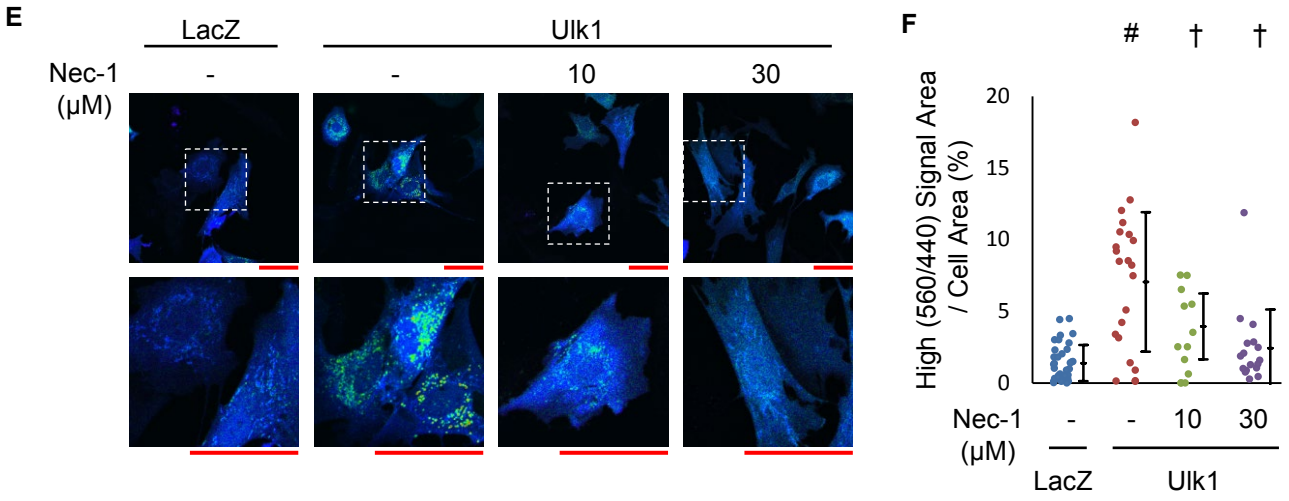

Supplemental Figure 8. Continued.

(E, F) The effect of 7-Cl-O-Nec-1 upon mitophagy induced by overexpression of Ulk1 was examined in CMs transduced with Mito-Keima.

(E) Representative images showing high ratio dots of Mito-Keima (scale bar, 50 μm).

(F) Quantitation of the area of high ratio dots/the total cell area.

The cell numbers in each group were 36 (LacZ) and 22, 13, 17 (Ulk1) from 3 independent experiments. Error bars represent SD. #$p<0.01$ vs. LacZ; †$p<0.01$ vs. Ulk1/Nec-1(-) (Tukey-Kramer's test).

Supplemental Figure 8

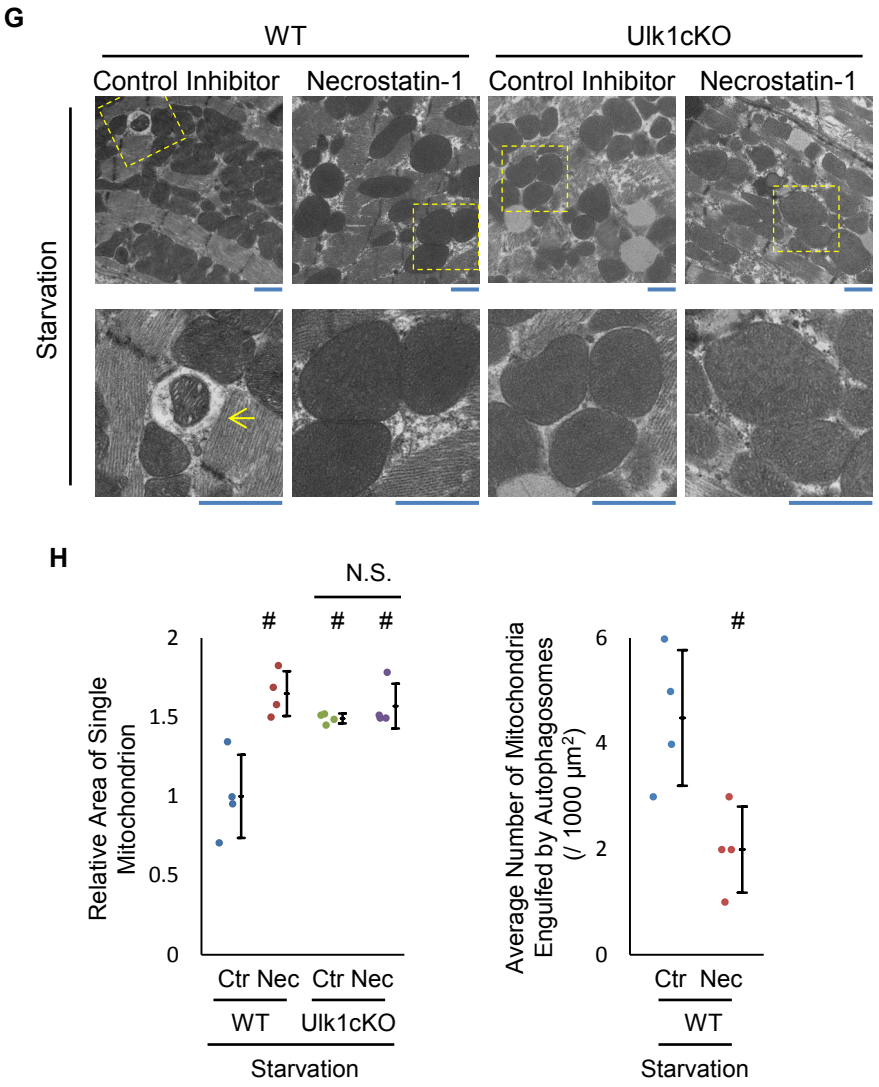

Supplemental Figure 8. Continued.

(G, H) Mice were subjected to 48-hour starvation. The effect of Necrostatin-1 upon mitochondrial fission and mitophagy in the heart was examined. Either control inhibitor or Necrostatin-1 (1.65 μg/g BW) was injected intraperitoneally twice during 48-hour starvation.

(G) Representative electron micrographs of the heart. Enlarged images are shown below (scale bar, 1 μm). An arrow (→) indicates the double membrane structure of an autophagosome.

(H) Quantitation of the average area of individual mitochondria (Upper) and the average number of mitochondria engulfed by autophagosomes (Lower) in the heart. At least 200 mitochondria were measured for each mouse (n=4 per group). Error bars represent SD. #p<0.01 vs. WT/Ctr; N.S. not significant (Tukey-Kramer's test (left panel), Student's t-test (right panel)).

Supplemental Figure 8

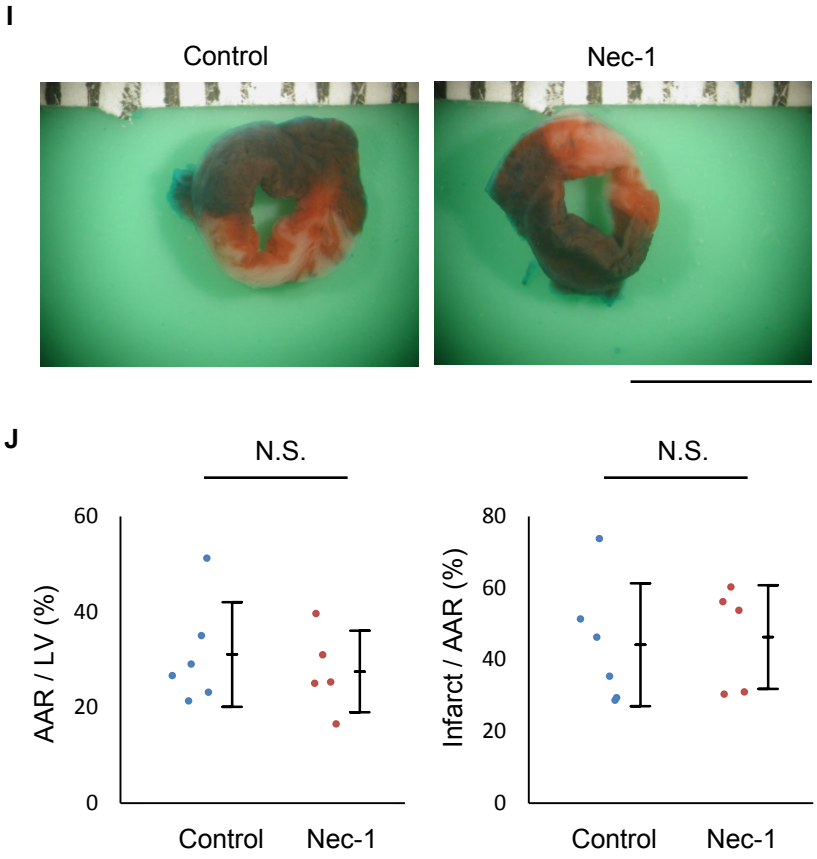

Supplemental Figure 8. Continued.

(I) Representative images of left ventricular (LV) slices with Alcian blue and triphenyltetrazolium chloride (TTC) staining (scale bar, 5 mm).

(J) Left: Area at risk (AAR)/LV. Right: Infarct size/AAR. n=5-6 per group. Error bars represent SD. N.S. not significant (Student's t-test (unpaired)).

Supplemental Figure 8

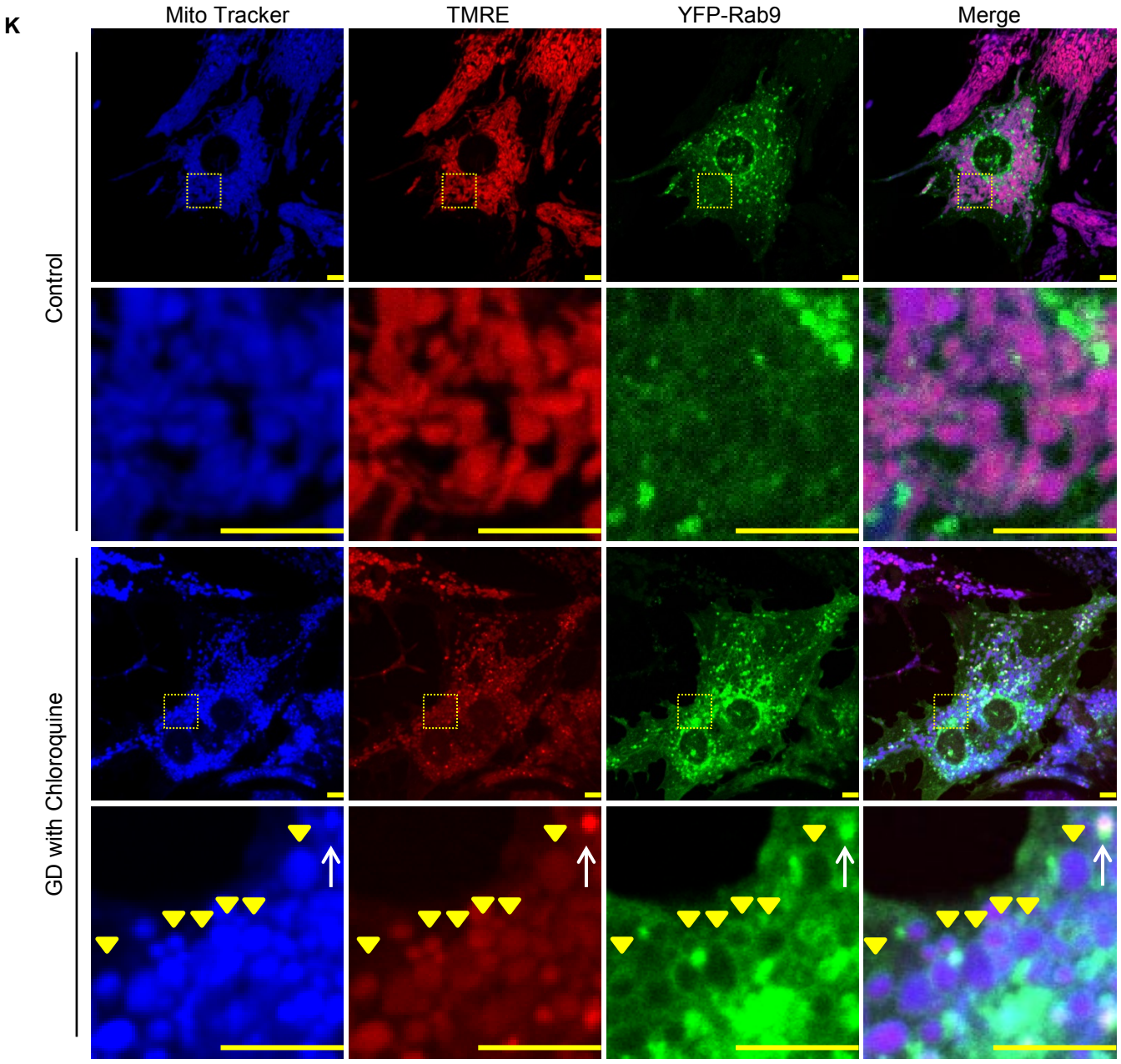

Supplemental Figure 8. Continued.

(K) Representative confocal micrographs of CMs transduced with YFP-Rab9 and stained with Mito Tracker Deep Red and TMRE. Enlarged images of areas indicated by rectangles are shown below (scale bar, 5 μm). Quantification and statistical analysis are shown in the lower panel. The analyses were conducted in 10 (Control) and 12 (GD with CQ) areas. Error bars represent SD. #p<0.01 vs. Pink (GD with CQ) (Student's t-test (unpaired)).

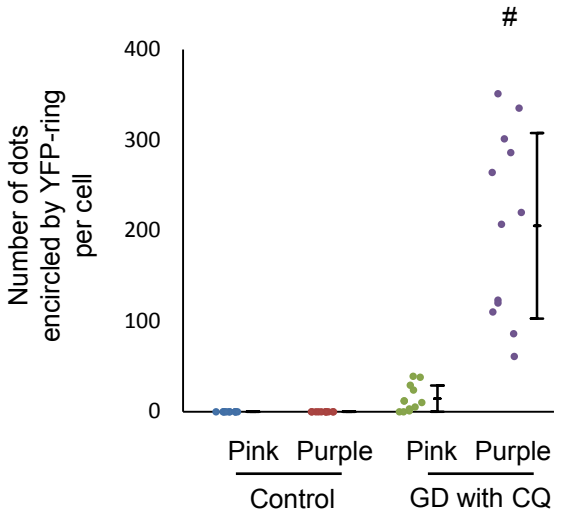

Supplemental Figure 9

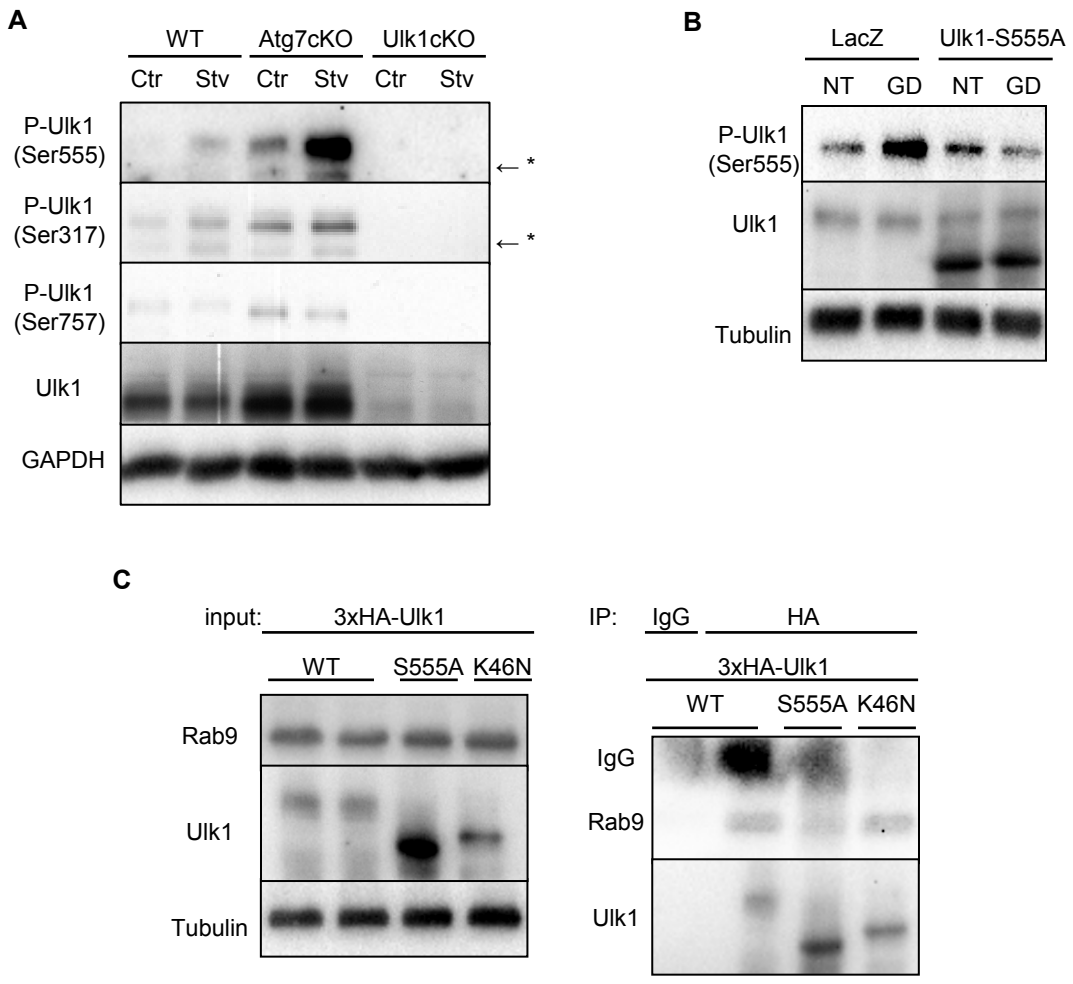

Supplemental Figure 9.

(A) Phosphorylation levels of Ulk1 in the heart were analyzed. Representative immunoblots are shown.

(B) Representative immunoblots showing phosphorylated Ulk1 (Ser555) and Ulk1 expression. Ulk1 was detected on a parallel gel using the same samples. NT: No treatment, GD: Glucose deprivation.

(C) Co-immunoprecipitation was conducted in cardiomyocytes (CMs) transduced with indicated adenoviruses, using anti-IgG or anti-HA antibody.

Supplemental Figure 9

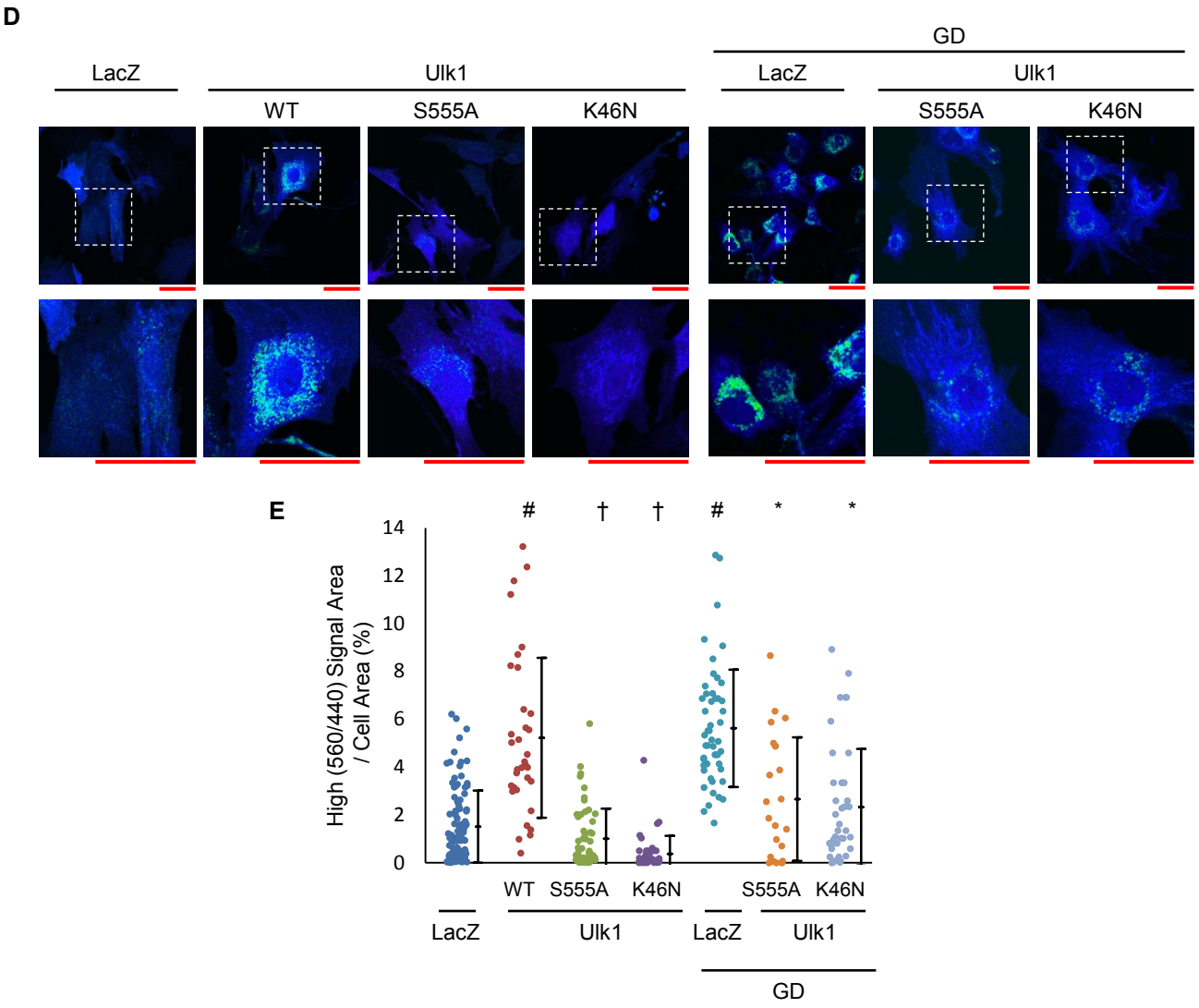

Supplemental Figure 9. Continued.

(D, E) The effect of mutant forms of Ulk1 (S555A and K46N) upon mitophagy was examined in CMs transduced with Mito-Keima.

(D) Representative images showing the high ratio dots. Enlarged images are shown below (scale bar, 50 μm).

(E) Quantitation of the area of high ratio dots/the total cell area. The cell numbers in each group were 53 (LacZ/NT), 34 (Ulk1 WT), 55 (Ulk1 S555A), 42 (Ulk1 K46N), 51 (LacZ/GD), 23 (Ulk1 S555A/GD), 40 (Ulk1 K46N/GD), from 3 independent experiments. Error bars represent SD. #p<0.01 vs. LacZ/NT; †p<0.01 vs. Ulk1 WT; *p<0.01 vs. LacZ/GD (Tukey-Kramer's test).

Supplemental Figure 9

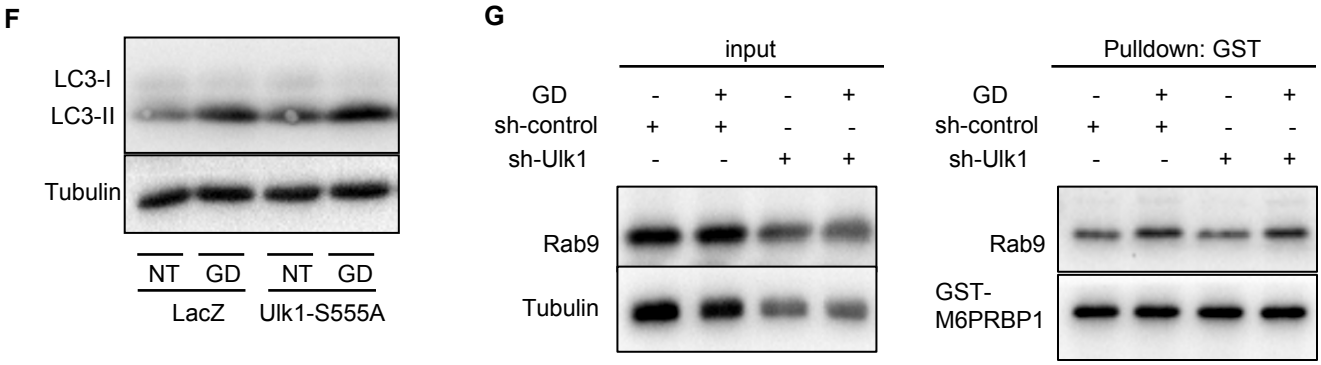

Supplemental Figure 9. Continued.

(F) Representative immunoblots showing LC3-I (top panel, upper band) and LC3-II (top panel, lower band) expression.

(G) Representative pull-down assay of Rab9 bound to GST-tagged M6PRBP1. In right panel, GST-M6PRBP1 was detected on a parallel gel using the same samples.

Supplemental Figure 9

H

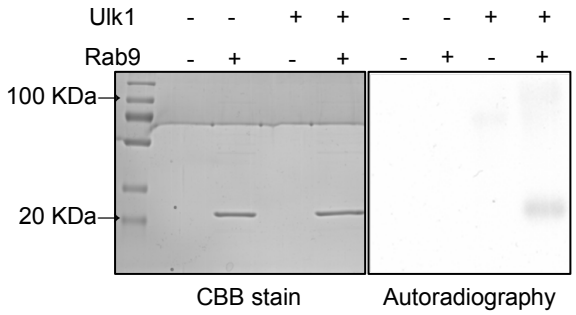

I

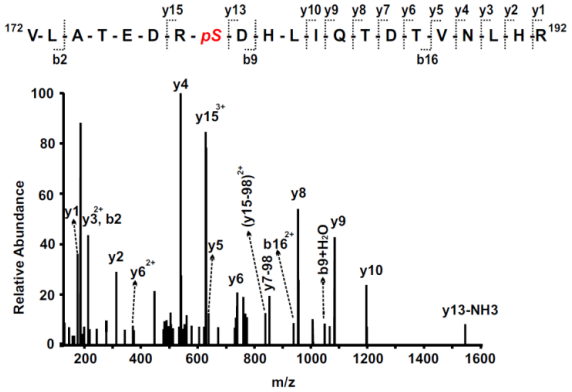

K

Homo sapiens	RVLATEDR**S**DHLIQT
Mus musculus	RILATEDR**S**EHLIQT
Rattus norvegicus	RILATEDR**S**DHLIQT
Canis lupus familiaris	RVLATEDR**S**DHLIQT
Bos taurus	RVLATEDR**S**DPLIQT
Xenopus laevis	RVLAIEDR**S**DQLIHT

J

	Peptide Sequence	Modification	phosphopeptide quantitation (Rab-9A)	phosphopeptide quantitation (Rab-9A + ulk1)
Ser179	RVLATEDRSDHLIQTDTVNLHR	S9(Phospho)	67.93%	99.92%
Thr175 or Ser179	VLATEDRSDHLIQTDTVNLHR *or* VLATEDRSDHLIQTDTVNLHR	T4(Phospho) *or* S8(Phospho)	43.10%	63.25%
Ser134	QVSTEEAQAWCRDNGDYPYFETSAK	S3(Phospho)	0.05%	2.04%
Ser5	aGKSSLFK	N-Term(Acetyl); S4(Phospho)	0.02%	1.92%
Ser21	VILLGDGGVGKSSLmNR	S12(Phospho); M15(Oxidation)	0.30%	0.03%
Ser187	SDHLIQTDTVNLHR	T9(Phospho)	0.85%	0.61%

Supplemental Figure 9. Continued.

(H) *In vitro* kinase assays were performed. Ten ng of recombinant Ulk1 (lane 3 and lane 4) and 1 µg of recombinant Rab9 (lane 2 and lane 4) were incubated with ATP at 30°C for 30 minutes. Left: A Coomassie-stained gel. Right: Autoradiograph.

(I) MS/MS spectrum of a 4+ ion (*m/z* 629.06) corresponding to the peptide sequence of **^{172}VLATEDR*p*SDHLIQTDTVNLHR^{192}** with a phosphorylation modification at Ser179. The observed ***y-*** and ***b-***ion series confirmed the peptide sequence and modification.

(J) The identified phosphopeptides and their relative abundance are listed.

(K) Conservation of Rab9 Ser179 across different species is shown.

Supplemental Figure 9

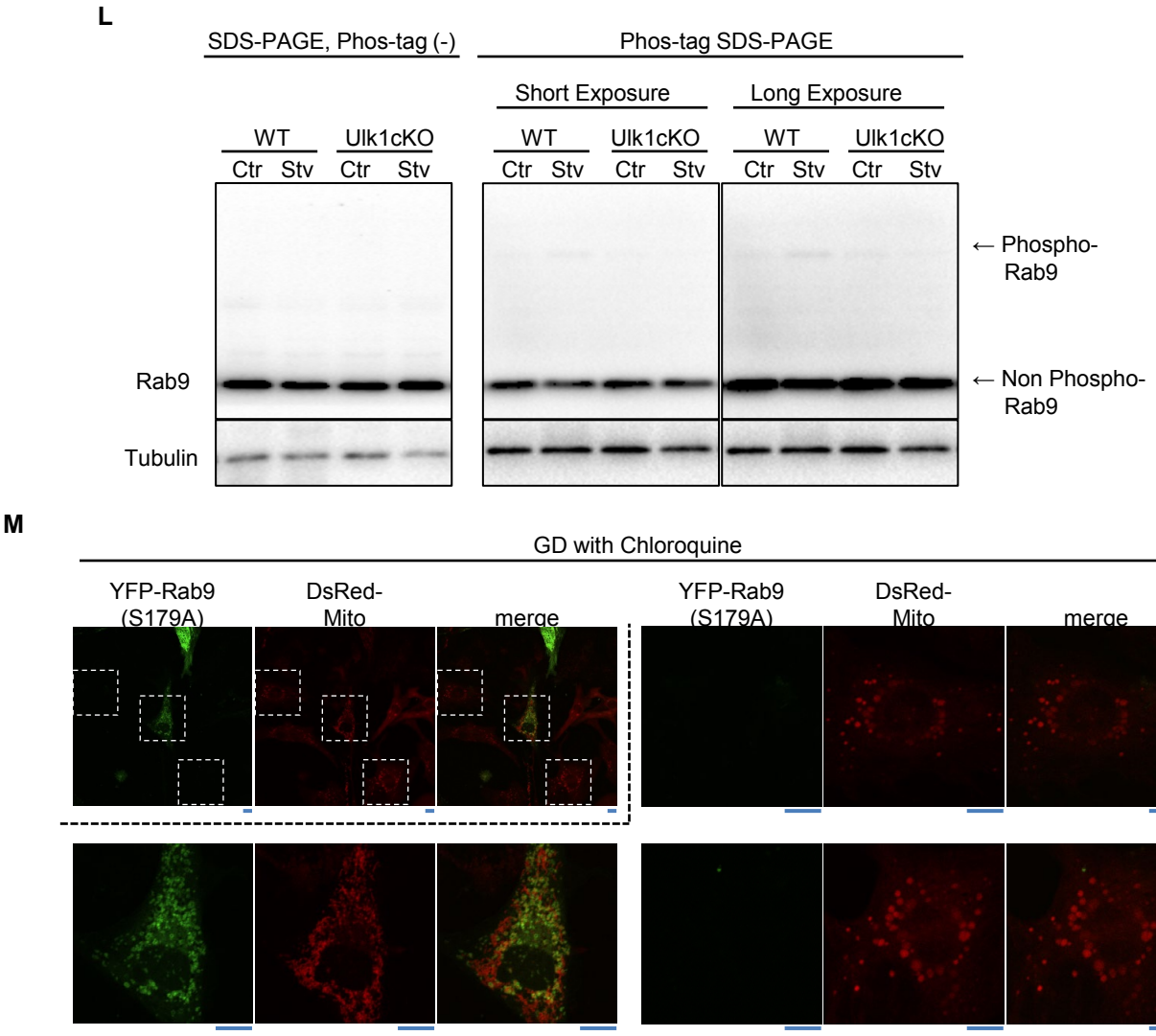

Supplemental Figure 9. Continued.

(L) Left: SDS-PAGE without Phos-tag. Anti-Rab9 antibody detected an intense band around the molecular weight of Rab9.

Right: SDS-PAGE with Phos-tag. Anti-Rab9 antibody detected an intense band corresponding to Rab9, indicating an unphosphorylated form of Rab9, in all 4 lanes. A band with a higher molecular weight was recognized in a Phos-tag-dependent manner, indicating a mono-phosphorylated form of Rab9. This upper band was stronger in lane 2 than in other lanes, suggesting that the mono-phosphorylation of Rab9 was upregulated by starvation and was downregulated by the genetic deletion of Ulk1.

(M) Representative confocal micrographs of CMs transduced with YFP-Rab9 (S179A) and DsRed-Mito during GD with chloroquine. Enlarged images of areas indicated by rectangles are shown below and right (scale bar, 10 μm). CMs expressing YFP-Rab9 (S179A) displayed tubular mitochondria, whereas the CMs without YFP signal exhibited round mitochondria, suggesting that the phospho-resistant mutant of Rab9 (S179A) inhibits mitochondrial fragmentation.

Supplemental Figure 10

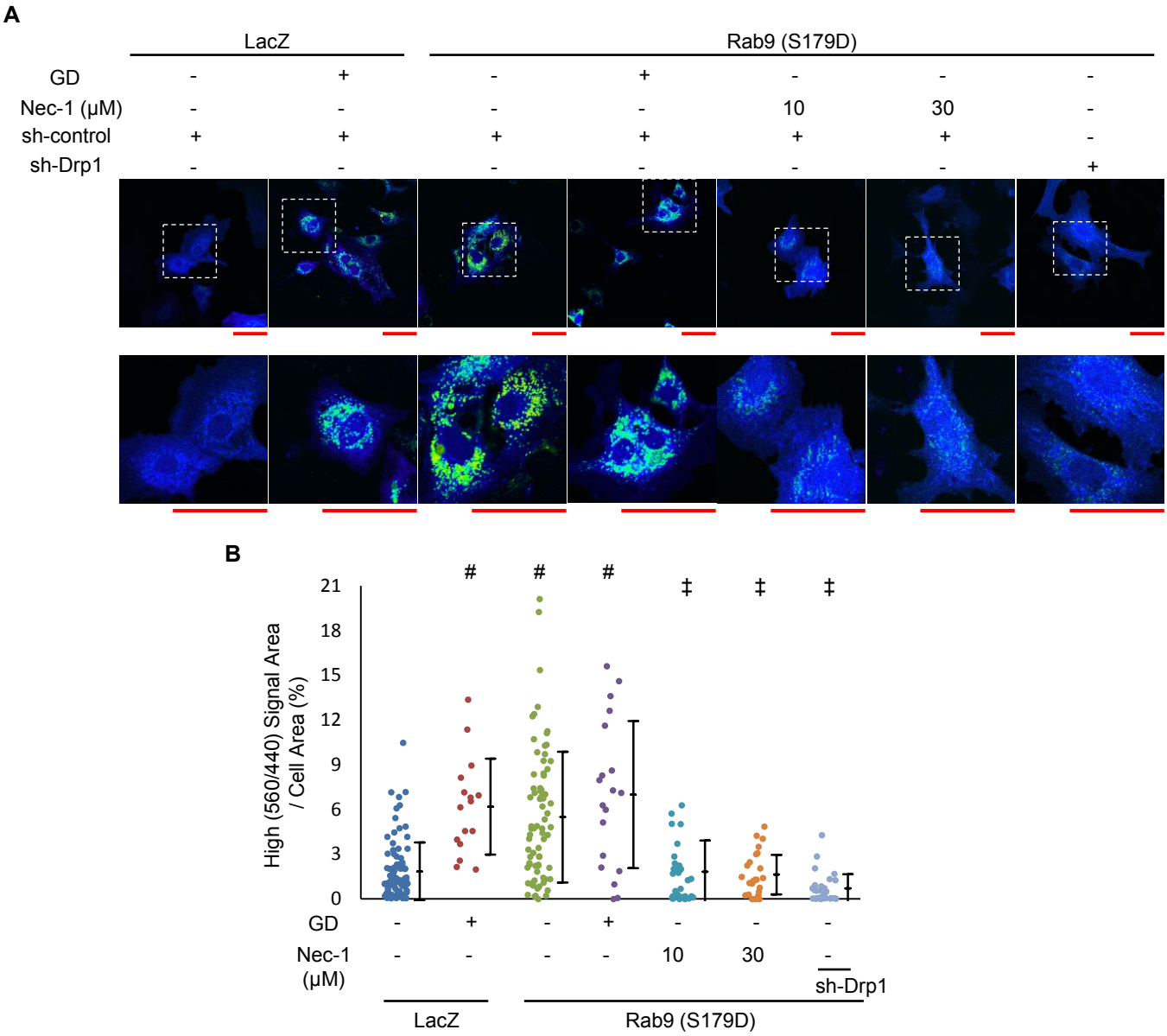

Supplemental Figure 10.

(A, B) The effect of overexpression of mutant forms of Rab9 upon mitophagy was examined in CMs transduced with Mito-Keima.

(A) Representative images showing high ratio dots of Mito-Keima. Enlarged images are shown below (scale bar, 50 μm).

(B) Quantitation of the area of high ratio dots/the total cell area.

The cell numbers in each group were 85, 16 (LacZ) and 66, 19, 32, 29, 31, 21 (Rab9(S179D)) from 3 independent experiments. Error bars represent SD. #p<0.01 vs. LacZ/NT; ‡p<0.01 vs. Rab9(S179D)/GD(-)/Nec-1(-) (Tukey-Kramer's test).

Supplemental Figure 10

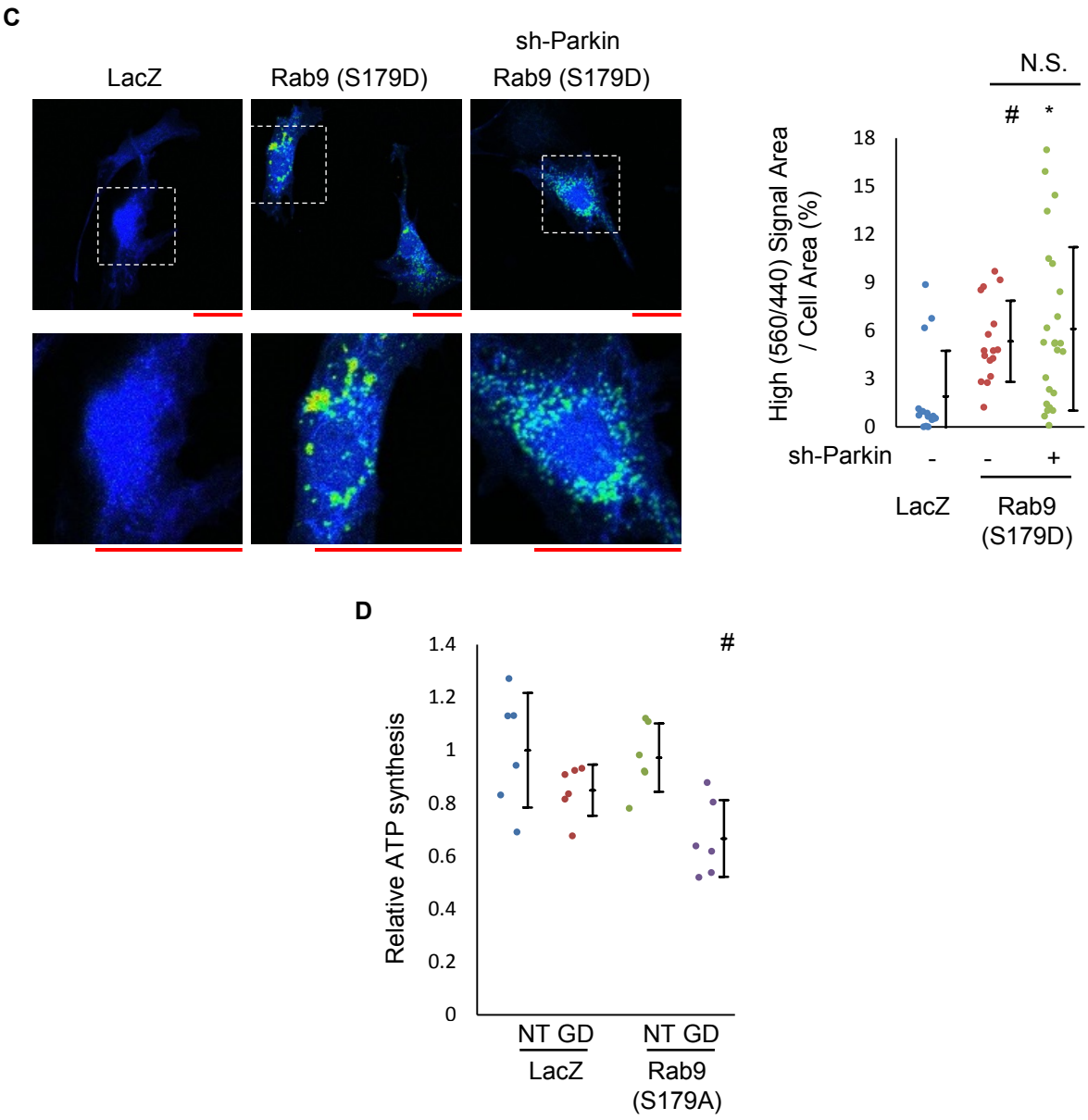

Supplemental Figure 10. Continued.

(C) The effect of knockdown of Parkin upon Rab9-mediated mitophagy was examined in CMs transduced with Mito-Keima. The cell numbers in each group were 15 (LacZ), 16 (Rab9 (S179D)) and 24 (Rab9 (S179D)/sh-Parkin). Error bars represent SD. #p<0.05 vs. LacZ; *p<0.01 vs. LacZ; N.S. not significant (Tukey-Kramer's test).

(D) ATP synthesis in mitochondria isolated from CMs transduced with LacZ or Rab9 (S179A) (n=6). Error bars represent SD. #p<0.05 vs. GD/LacZ (Student's t-test (unpaired)).

Supplemental Figure 11

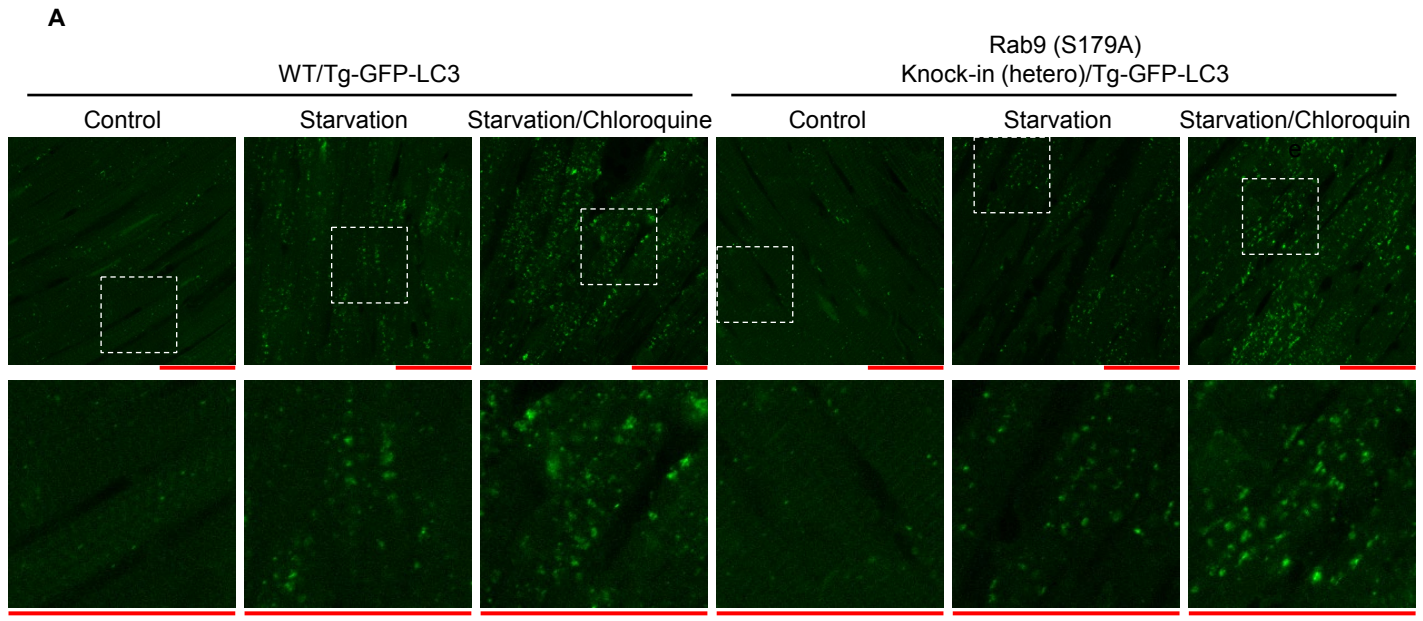

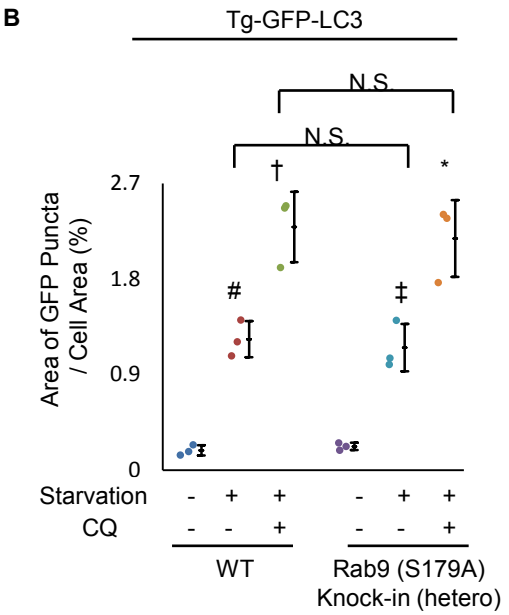

Supplemental Figure 11.

(A, B) Autophagic flux was analyzed in the hearts of Tg-GFP-LC3 mice after chloroquine administration (10 μg/kg i.p.) during 48-hour starvation. Representative images are shown in (A) (scale bar, 50 μm). Summary is shown in (B) (n=3 per group). CQ: Chloroquine. Error bars represent SD. N.S. not significant; #p<0.01 vs. WT/Ctr; †p<0.01 vs.WT/Stv/CQ(-); ‡p<0.01 vs. Rab9 Knock-In/Ctr; *p<0.01 vs. Rab9 Knock-In/Stv/CQ(-) (Tukey-Kramer's test).

Supplemental Figure 11

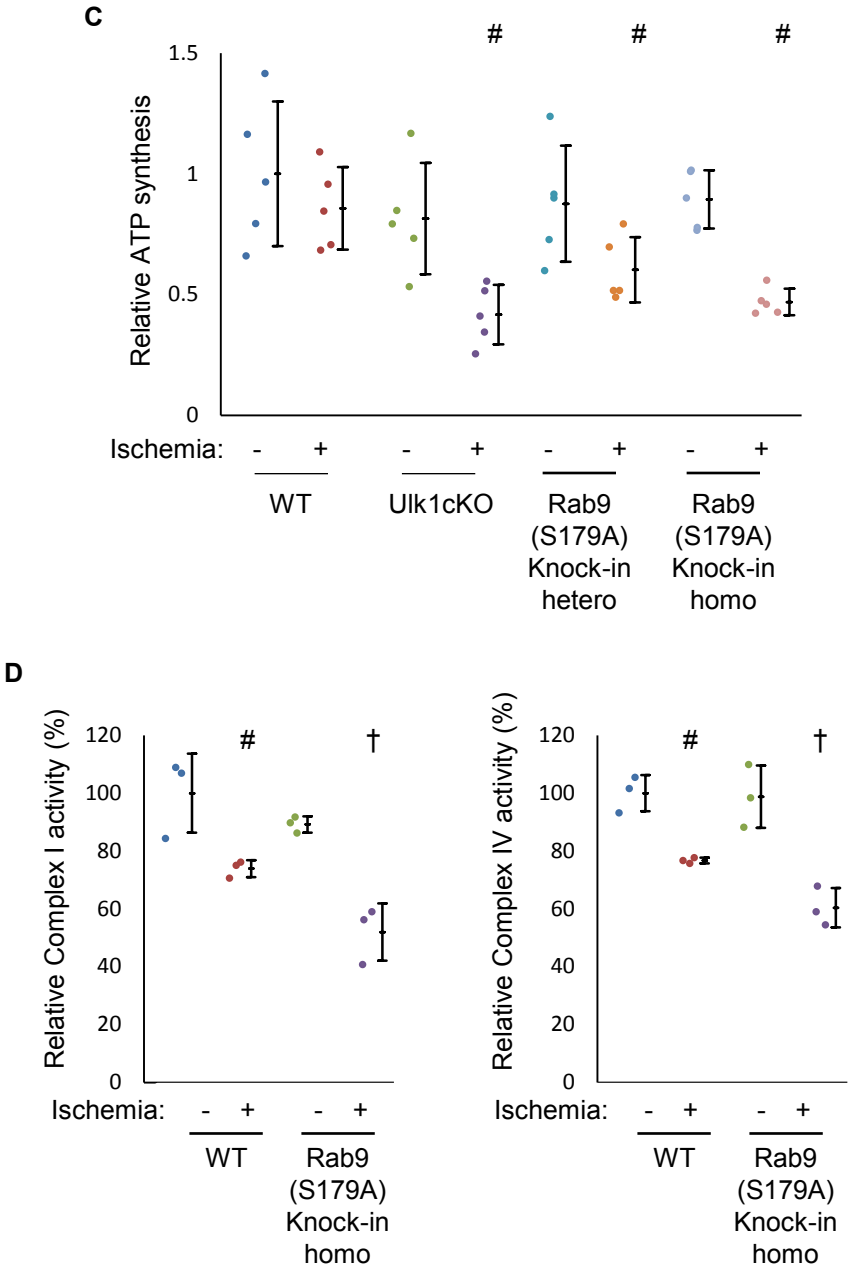

Supplemental Figure 11. Continued.

(C) ATP synthesis in mitochondria isolated from the heart (n=5). Error bar represents SD. #p<0.05 vs. Ischemia (+)/WT (Student's t-test (unpaired)).

(D) The activity of complex I and IV in mitochondria isolated from the heart (n=3). Error bar represents SD. #p<0.05 vs. ischemia (-)/WT; †p<0.05 vs. ischemia (+)/WT (Student's t-test (unpaired)).

Supplemental Figure 11

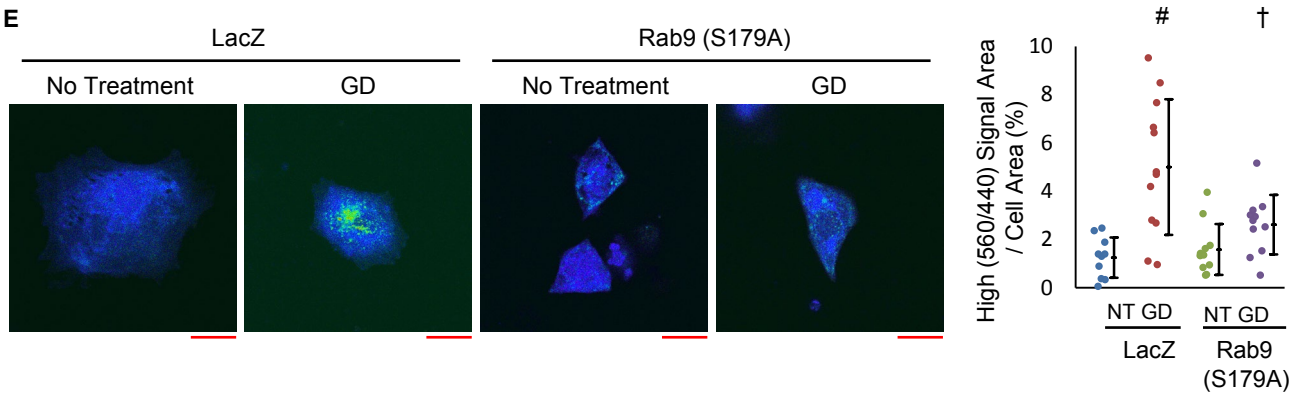

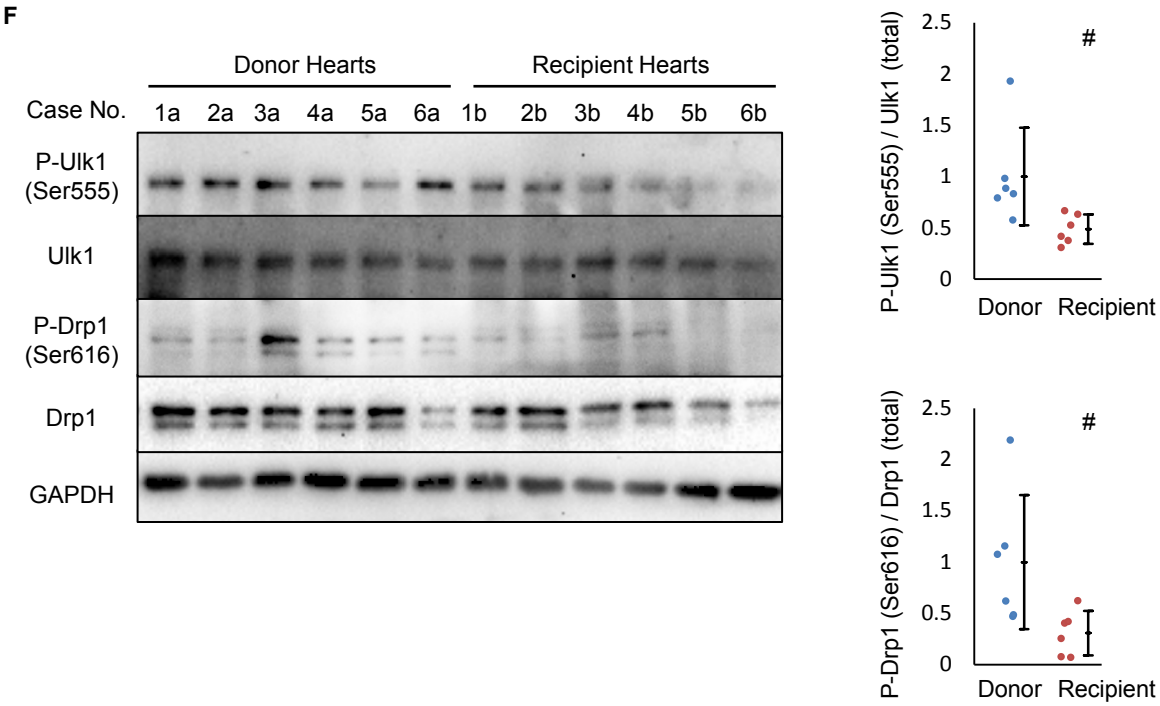

Supplemental Figure 11. Continued.

(E) Human induced pluripotent stem cells (hiPSCs) were differentiated into beating cardiomyocytes (hiPSC-CMs) as described previously [33]. Lysosomal degradation of mitochondria was examined in hiPSC-CMs transduced with Mito-Keima and subjected to 4 hours of glucose deprivation. Lactate- but not glucose-containing medium was used for this condition. (left) Representative images showing high ratio (560 nm/440 nm) dots representing mitophagy (scale bar, 50 μm). (right) Quantitation of the area of high ratio dots per cell area (%), evaluated as a measure of mitophagy. The cell numbers in each group were 10-13. Error bars represent SD. #p<0.01 vs. LacZ/NT; †p<0.05 vs. LacZ/GD (Tukey-Kramer's test).

(F) Immunoblot analyses of myocardial tissue homogenates from explanted human hearts with indicated antibodies. Six samples (cases 1b-6b) were from heart transplant recipients and six samples (cases 1a-6a) were from heart donors. Representative blots are shown in left. Summaries are shown in right (n=6 per group). Error bars represent SD. #p<0.05 vs. Donor (Student's t-test (unpaired)).

Supplemental Figure 11

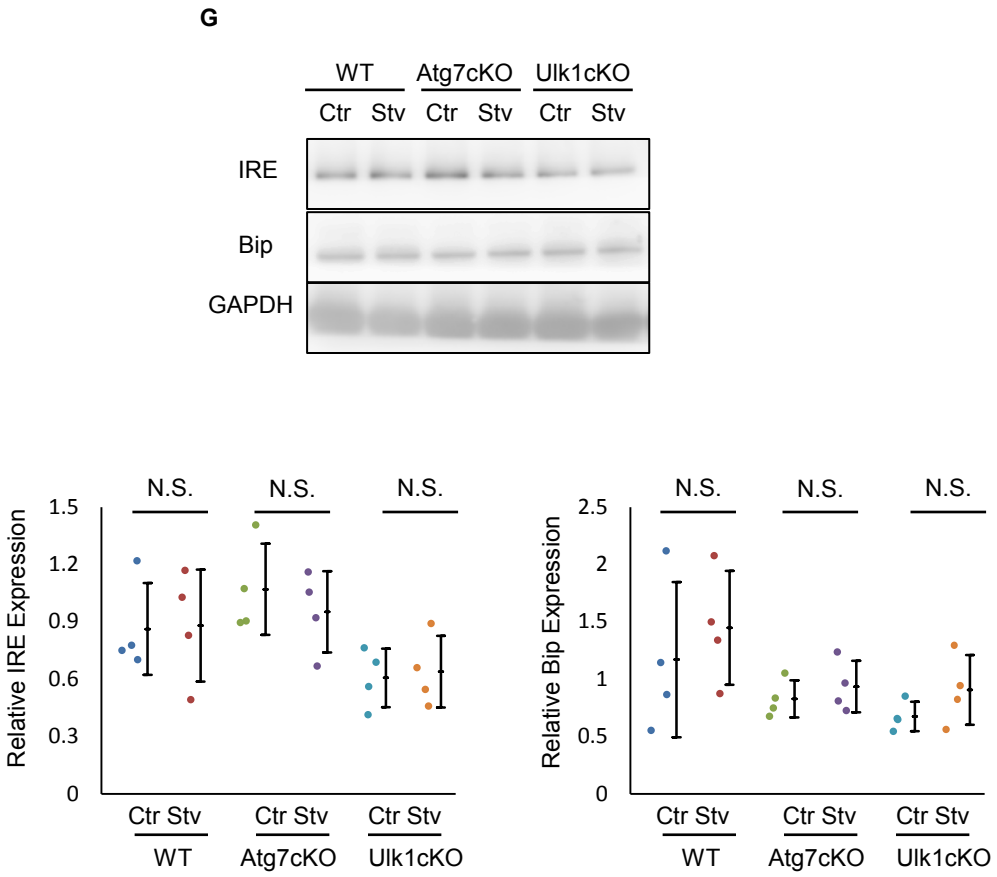

Supplemental Figure 11. Continued.

(G) Mice were subjected to 48-hour starvation. Ctr: control, Stv: starvation. Error bars represent SD. Protein levels of ER markers in the heart were analyzed. IRE was detected on a parallel gel using the same samples. Representative immunoblots, quantification and statistical analysis are shown (n=4 per group). N.S. not significant (Student's t-test (paired)).

Supplemental Table 1

A list of the characteristics of the heart transplant recipients and donors enrolled in the experiments of Supplemental Figure 11F.

Donors			Recipients			
Case No.	Age*	Sex	Case No.	Age*	Sex	Diagnosis
1a	66	M	1b	48	M	Dilated Cardiomyopathy
2a	48	M	2b	57	M	Dilated Cardiomyopathy
3a	51	M	3b	52	M	Dilated Cardiomyopathy
4a	57	M	4b	74	F	Dilated Cardiomyopathy
5a	68	M	5b	48	M	Dilated Cardiomyopathy
6a	44	F	6b	45	M	Dilated Cardiomyopathy

* Mean ± SEM = 55.7 ± 4.0

* Mean ± SEM = 54.0 ± 4.3